

Filling the ceratosaur gap: A new ceratosaurian theropod from the Early Cretaceous of Spain

BÁRBARA SÁNCHEZ-HERNÁNDEZ and MICHAEL J. BENTON



Sánchez-Hernández, B. and Benton, M.J. 2014. Filling the ceratosaur gap: A new ceratosaurian theropod from the Early Cretaceous of Spain. *Acta Palaeontologica Polonica* 59 (3): 581–600.

Ceratosaurian theropods evolved in two bursts, first in the Middle and Late Jurassic and then in the Late Cretaceous, leaving a 20 Myr gap in the Early Cretaceous during which remains are rare. We describe here a new ceratosaurian theropod, *Camarillasaurus cirugedae*, from fluvial deposits of the Camarillas Formation (lower Barremian, Lower Cretaceous) of Camarillas, Teruel Province, NE Spain. The new theropod is represented by a collection of associated bones, including a tooth, a possible cervical vertebra, two sternal plates, the proximal part of a right tibia, a broken right scapulocoracoid, the incomplete sacrum, five caudal vertebrae, an isolated caudal neural arch, a chevron, an almost complete presacral rib and some fragments of vertebrae, ribs, and other elements. *Camarillasaurus* is differentiated from other theropods by the extreme depth of the tibia proximal end, and a deep longitudinal groove on the tibia. The new dinosaur is a ceratosaur, phylogenetically close to the base of the clade, and perhaps more derived than the Chinese basal ceratosaur *Limusaurus*. The new taxon is significant in the evolution of the ceratosaurian dinosaurs, being placed temporally between its more common Jurassic and mid-Upper Cretaceous relatives, and it is one of only a few from Laurasia.

Key words: Dinosauria, Theropoda, Ceratosauria, Barremian, Cretaceous, Teruel Province, Aragón, Spain.

Bárbara Sánchez-Hernández [bshdez@hotmail.com] and Michael J. Benton [Mike.Benton@bristol.ac.uk] (corresponding author), School of Earth Sciences, University of Bristol, Queens Road, Bristol, BS8 1RJ, United Kingdom.

Received 12 September 2012, accepted 18 October 2012, available online 23 October 2012.

Copyright © 2014 B. Sánchez-Hernández and M.J. Benton. This is an open-access article distributed under the terms of the Creative Commons Attribution License, which permits unrestricted use, distribution, and reproduction in any medium, provided the original author and source are credited.

Introduction

The Ceratosauria were theropod dinosaurs known from the Middle Jurassic to Late Cretaceous, predominantly from southern continents, and coeval with their larger sister clade, the Tetanurae. Their phylogeny has been debated, but the clade is now widely seen as excluding coelophysoids (Carrano and Sampson 2008). The temporal distribution of ceratosaurs (Pol and Rauhut 2012) includes a diversity of Middle and Late Jurassic and mid to Late Cretaceous forms with a substantial time gap between, termed here the “ceratosaur gap”, that lasted at least from Berriasian to Barremian, a span of 20 Myr. Even in the mid Cretaceous (Aptian and Albian), ceratosaurs are still poorly documented. The time-tree of Pol and Rauhut (2012) shows two radiations of ceratosaurs, the first in the Middle and Late Jurassic, and the second at the base of the Late Cretaceous, with only four lineages crossing the Early Cretaceous, one each for *Deltadromeus* and *Genyodectes*, and one each running to the bases of the subclades Noasauridae and derived Abelisauridae.

Jurassic ceratosaurs include the Middle Jurassic abelisaurid *Eoabelisaurus* from Argentina (Pol and Rauhut 2012),

the Late Jurassic *Ceratosaurus* (Marsh 1884), *Elaphrosaurus* (Janensch 1920), and *Limusaurus* (Xu et al. 2009) from North America, Africa, and Asia, respectively. A supposed abelisauroid from the Middle Jurassic of England (Ezcurra and Agnolin 2012) has been re-evaluated (Rauhut 2012) as possessing no clear apomorphies of the clade. Mid-Cretaceous (Aptian–Albian) ceratosaurs include *Genyodectes* from South America (Rauhut 2004), *Kryptops* from Africa (Serenó and Brusatte 2008), and *Genusaurus* (Accarie et al. 1995; Carrano and Sampson 2008) from France. Late Cretaceous ceratosaurs include *Rugops*, and *Deltadromeus* from North Africa, *Abelisaurus*, *Aucasaurus*, *Carnotaurus*, *Ilokelesia*, *Noasaurus*, *Skorpiovenator*, and *Xenotarsosaurus* from South America, *Majungotholus*, and *Masiakasaurus* from Madagascar, *Indosaurus*, *Indosuchus*, and *Rajasaurus* from India, and the uncertain genera *Tarascosaurus* from France and *Betasuchus* from the Netherlands (Carrano et al. 2002, 2011; Sereno et al. 2004; Tykoski and Rowe 2004; Carrano and Sampson 2008; Canale et al. 2009).

The “ceratosaur gap” is not entirely devoid of ceratosaur fossils, but remains are incomplete (Carrano and Sampson 2008: fig. 5). These are the possible abelisauroid *Ligabueino andesi* from the La Amarga Formation (Barremian) of Argen-

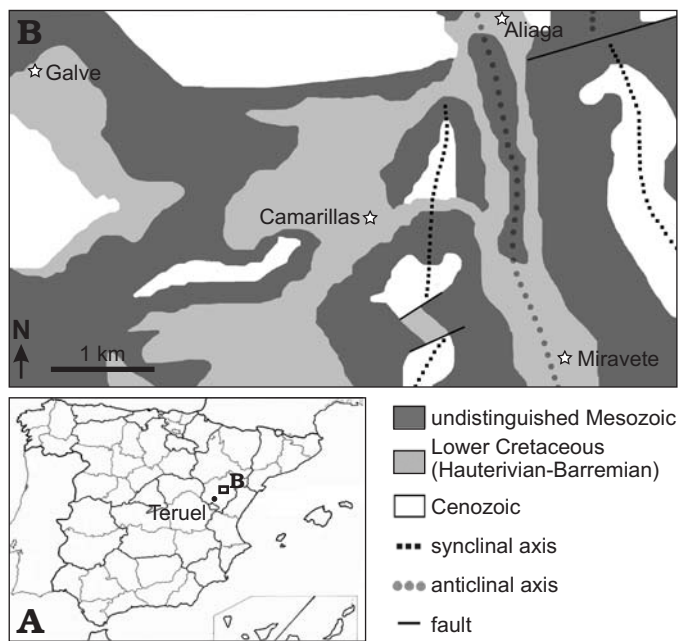


Fig. 1. Geographic and geological setting of the Camarillas area, Teruel Province, Aragón, north-east Spain, showing general location (A), and simplified geological map (B), highlighting the major sedimentary units and structures. Fossiliferous localities, including Camarillas, marked with open stars. Based on Soria (1997).

tina which has generally been regarded as poorly diagnostic, if not a *nomen dubium* (Carrano et al. 2002; Tykoski and Rowe 2004; Sereno and Brusatte 2008), the possible abelisauroid (Sereno et al. 2004) *Spinostropheus* (*Elaphrosaurus*) *gautieri*, based on cervical and dorsal vertebrae from the Tiourarén Formation (?Hauterivian) of Niger, and teeth from the Cerro Barcino Formation of Argentina assigned to “Abelisauria indet.” (Rauhut et al. 2003). There are also various disputed Early Cretaceous (Aptian–Albian) possible ceratosaur remains from Australia (reviewed by Benson et al. 2012), and a definite ceratosaur astragalus (Fitzgerald et al. 2012).

This scattered geographic and temporal distribution has been explained by two hypotheses: first, it could be that ceratosaurs achieved a wide distribution during the existence of Gondwana, but their fossils are not yet known in certain areas until the Late Cretaceous (Lamanna et al. 2002; Calvo et al. 2004; Sereno et al. 2004); or second, they actually achieved a widespread distribution during the Jurassic and again in the Late Cretaceous, were genuinely rare in the Early Cretaceous, and struggled to reach Gondwana at all times because of a major geographic barrier (Pol and Rauhut 2012). The apparent rarity of ceratosaurs in Australia may be a climatic effect because that continent experienced cold, high-latitude conditions when compared with much of the rest of Pangaea (Benson et al. 2012). Further, Pol and Rauhut (2012) suggest that abelisauroids were largely restricted to southern Gondwana during the Jurassic and Cretaceous because the central Gondwanan desert formed a barrier, and few reached Laurasia, except Europe.

Here, we describe a new ceratosaurian dinosaur from the

Early Cretaceous (early Barremian) of Spain, which is the first ceratosaurian from the earliest Cretaceous of Europe, and a contribution to filling the “ceratosaur gap”. Indeed, this is the first report also of vertebrate remains from the Camarillas locality (Teruel Province, Aragón, NE Spain).

Institutional abbreviations.—MPG, Museo Paleontológico de Galve, Galve village (Teruel Province), Spain. The collection is termed MPG-KPC, based on the locality (K, Camarillas) and finder (PC, Pedro Cirujeda).

Geological setting

The bones of the new dinosaur were found associated with remains of other dinosaurian taxa, including a small theropod and isolated coprolites. The fossils come from a rock outcrop in a farm field, which, according to the discoverer of the dinosaur remains, is called Fuente Arnar, within the land of the Pedro Cirujeda Buj family, close to Camarillas village. The fossils are disarticulated, but they were all found at the same time and within an area of approximately five square metres during ploughing.

The Camarillas locality is 10 km from Galve, a small village at the centre of an area that has yielded numerous Late Jurassic–Early Cretaceous vertebrate remains (Sánchez-Hernández 2002, 2005; Sánchez-Hernández et al. 2007). Because of their close proximity, all the formations described from the Galve area are also found in the Camarillas area. They are in the following stratigraphic order from the bottom (Palaeozoic basement) to the top: Higuieruelas Formation (Upper Jurassic), Villar del Arzobispo Formation (Upper Jurassic–lower Berriasian), El Castellar Formation (Hauterivian–Barremian), Camarillas Formation (Barremian), and Artoles Formation (upper Barremian–lower Aptian). A detailed account of the different units and the fossil remains preserved in them can be found in Sánchez-Hernández et al. (2007).

Both Camarillas and Galve are in the Galve Subbasin, a section of the Aliaga Basin, in the Iberian Range. All these basins were formed during the Permian–Triassic, when the main faults were active (Arche and López-Gómez 1996), and they are filled with Mesozoic–Quaternary sediments (Fig. 1). The Upper Permian–Upper Jurassic deposits are all of continental origin. In a second extensional stage during the Late Jurassic–Early Cretaceous, the Atlantic and the Bay of Biscay opened, and the Iberian Peninsula rotated from left to right (Gong et al. 2009). At this time, the sediments were marine or showed the influence of the sea, as shown in the deposits of the Higuieruelas and Villar del Arzobispo formations in the Galve Subbasin. Finally, during the Early Cretaceous and Oligocene–Miocene there were compressive phases with tectonic inversion and formation of continental basins (Salas and Casas 1993; Arche and López-Gómez 1996; Gong et al. 2009).

Camarillas village is located on Lower Cretaceous (Hauterivian–Barremian) deposits of the El Castellar and Camarillas formations (Fig. 1), and the new fossil outcrop

reported here is in the Camarillas Formation, in beds of similar age to the La Maca outcrop in the Galve area where the remains of an iguanodontid dinosaur have been found. The Camarillas fossil site is in light brown clay and limestone rocks with fossil wood remains. The sedimentology is similar to that described in the Galve area, because the Camarillas Formation shows scarcely any lateral variations in facies within the Galve Subbasin (Soria 1997).

The Camarillas Formation sandstone is fluvial, and four groups of palaeochannels are distinguished, the first towards the bottom of the succession. These channels become thinner towards the top, and this was interpreted by Díaz and Yébenes (1987) as evidence that there was an alluvial fan with a multichannel system. The lithology of the deposits which fill these channels and their geometry are typical of low-sinuosity channels. Towards the top of the Camarillas Formation, there is a predominance of deltaic fan deposits with marked marine influence (Díaz and Yébenes 1987). Nevertheless, Soria (1997) mentioned that she found no facies association whose evolution and geometry suggested a well developed deltaic system.

Systematic palaeontology

Superorder Dinosauria Owen, 1842

Order Saurischia Seeley, 1887

Suborder Theropoda Marsh, 1881

Infraorder Ceratosauria Marsh, 1884

Genus *Camarillasaurus* nov.

Etymology: From Camarillas, the name of the locality and formation where the bones were found, and *saurus*, reptile.

Type species: *Camarillasaurus cirugedae* sp. nov., monotypic; see below.

Diagnosis.—As for the type and only species.

Camarillasaurus cirugedae sp. nov.

Figs. 1–11.

Etymology: The species name *cirugedae* comes from the surname of the person, who found the bones, Pedro Cirugeda Buj.

Holotype: Specimen MPG-KPC1-46, a partial tooth, and associated isolated vertebrae, ribs, and limb elements. The close physical association of all the bones, their corresponding sizes, and independent evidence of ceratosaurian and/or abelisauroid characters in each (see Description below) suggest that all come from one taxon and one individual. In detail, the holotype consists of the apical part of a lateral tooth (MPG-KPC43), two almost complete sternal plates (MPG-KPC1, 2) and isolated remains of sternal plates (MPG-KPC34–38), a broken right scapulocoracoid (MPG-KPC23, 30), an almost complete presacral rib (MPG-KPC7), some rib fragments (MPG-KPC45 and 47–50), a posterior cervical or anterior dorsal vertebra (MPG-KPC9), an almost complete mid-dorsal vertebra (MPG-KPC21), two broken dorsal centra (MPG-KPC20 and 17), a broken sacrum (MPG-KPC3, 4), two sacral vertebral centra (MPG-KPC16, 18), an isolated neural arch (MPG-KPC39), a broken portion of a lateral side of a centrum with prezygapophysis (MPG-KPC51), three broken anterior caudal verte-

bral centra (MPG-KPC14, 15, 19), four mid-posterior caudal vertebrae (MPG-KPC10–13), a broken posterior caudal centra (MPG-KPC46), a broken portion of a vertebral centrum (MPG-KPC22), three possible broken tops of neural spines (MPG-KPC31–33), an almost complete chevron (MPG-KPC5, 6), an isolated broken blade of a chevron (MPG-KPC44), a proximal part of a right tibia (MPG-KPC8), and several isolated broken fragments of bones.

Type locality: Fuente Arnar outcrop, near Camarillas village, Teruel Province, Aragón, NE Spain.

Type horizon: Light brown clay and limestone beds, in which fossil wood remains are common, of the Camarillas Formation, lower Barremian, Lower Cretaceous (Díaz and Yébenes 1987; Sánchez-Hernández et al. 2007).

Diagnosis.—A ceratosaur (see Discussion) with the following two autapomorphies: extremely broad tibia proximal end, with ratio of anteroposterior/mediolateral axis of 2.8 (the highest of any theropod); tibia with a central narrow deep longitudinal groove placed anterolaterally to the crista fibularis on the medial surface which gives a g-shaped cross-section to the tibial shaft. Other characters include the chevron with a deep broad longitudinal groove along the length of the shaft arising from a fossa placed below the haemal canal on the anterior and posterior side; presence of an articular surface on the distal end of the chevron blade; caudal vertebrae with articular surfaces that have well developed edges and are unusually broad.

Geographic and stratigraphic range.—Type locality and horizon only.

Description

Tooth.—MPG-KPC43 is a broken apical fragment of a tooth that was found on the surface of the field where all the *Ca-*

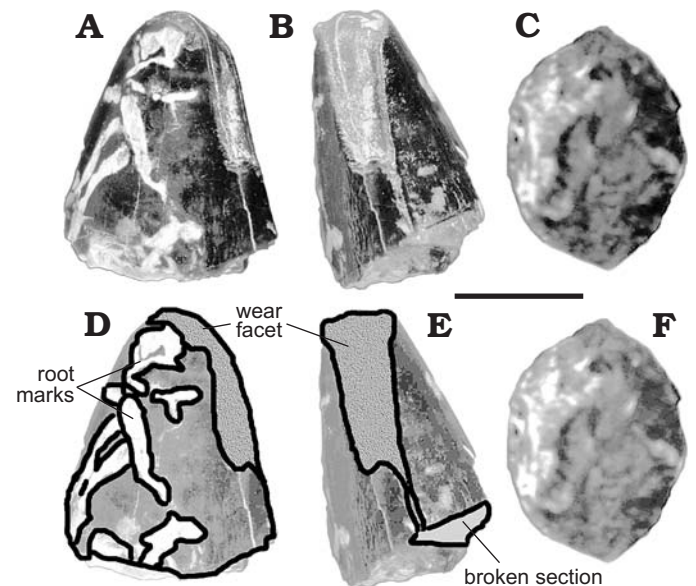


Fig. 2. Ceratosaurian theropod *Camarillasaurus cirugedae* gen. et sp. nov. from the Camarillas Formation of Camarillas, Soria Province, Spain, tooth, MPG-KPC43, in labial-lateral (A, D), lateral (B, E), and cross-sectional (C, F) views. The different damaged areas are marked (D, E), in clear grey for a broken section, dark grey for the wear facets, and white, for the root marks that have dissolved the enamel. Scale bar 5 mm.

marillasaurus remains were found, together with a broken piece of a vertebral centrum. The apical tooth fragment (MPG-KPC43; Fig. 2) has straight edges, although one side (probably distal) is more inclined than the other. The total height is 11 mm, mesiodistal length 9 mm, and labiolingual width 6.5 mm measured on the preserved oval-shaped base, giving a length/width ratio of 1.4. Assuming that the tooth was inclined labially, it is probably either a right maxillary tooth or a left dentary tooth. The bottom view of the tooth shows that the lingual surface is flatter than the labial, which is more convex (Fig. 2C). The crown is symmetrical.

Both surfaces (labial and lingual) of the broken tooth show white ridges caused by the roots of some modern plants that damaged and dissolved the enamel.

The tooth has a carina on the mesial and distal edges, as seen in the cross section of the base (Fig. 2C). At the apex and along the distal carina there is an ellipsoidal wear facet, concave in section (Fig. 2A, B, D, E). Although the enamel is not ornamented, the lingual surface shows weak vertical wrinkles under perpendicular light. These wrinkles have been lost on the labial face, where the marks made by roots are more acute (Fig. 2A, D). It is possible that the tooth bore longitudinal ridges lower down, in the unpreserved part, based on a comparison with dentary teeth of *Ceratosaurus* (Madsen and Welles 2000: figs. 2, 11), whose crowns show less clearly marked longitudinal ridges in the apical part than lower down. The enamel over the carina on the proximal side in MPG-KPC43 is lost. Consequently, although the carinae have no serrations, it is not possible to be sure whether serrations were originally present or not.

Theropod teeth, especially when incomplete, can be hard to identify (Smith 2012). Smith et al.'s (2012) study, based on comparison of selected measurements, allows discrimination of genera and families, but major clades, such as ceratosaurs and tetanurans, show broad overlaps in morphospace. MPG-KPC43 has an oval-shaped cross section, which is less laterally compressed than in many tetanurans, but is not so rounded as in spinosauroids (Brusatte et al. 2007). Tyrannosaurid teeth differ in the position of the carinae (Lamanna et al. 2002), the D-shaped cross-section (in premaxillary teeth), and the location of the wear facet never being over the mesial or distal surfaces (Schubert and Ungar 2005).

The Camarillas tooth shows ceratosaurian synapomorphies. For example, Rauhut (2004) suggested the flat or even slightly concave area near the marginal carinae in the lateral teeth is a possible ceratosaurian synapomorphy shared by *Ceratosaurus* and some abelisaurids such as *Majungasaurus*, and it is present in MPG-KPC43, especially towards its base, and in the middle part of the crown. *Majungasaurus* teeth share with MPG-KPC43 the cross-sectional shape and one side more inclined than the other, although they differ in the well-developed denticles (Rogers et al. 2003: figs. 2, 4). *Rugops primus* also seems to have symmetrical crowns with carinae on the proximal and distal edges and oval-shaped cross-section (Serenio et al. 2004: fig. 3d), and these teeth also share with MPG-KPC43 the presence of a

surface (possibly lingual in the tooth from Camarillas) flatter than the other (possibly labial), as has been also described for *Genyodectes* and *Ceratosaurus* (Rauhut 2004), for teeth in the Cenomanian abelisaurid maxilla UCPC10 from Morocco (Mahler 2005: fig. 1), and for *Skorpiovenator* (Canale et al. 2009). Teeth of *Skorpiovenator* show arcuate (horizontal) enamel wrinkles, different from other abelisaurids. The teeth of *Kryptops palaios* (Serenio and Brusatte 2008: fig. 8) are also quite similar to MPG-KPC43, sharing similar slight ornamentation of the enamel, scarcely compressed cross section, carinae with lower denticles than in *Masiakasaurus* and a well developed wear facet located over a carina. Based on these common features, MPG-KPC43 is considered to belong to a ceratosaur dinosaur.

Axial skeleton

Cervical vertebrae.—An isolated specimen, MPG-KPC24 (Fig. 3), may belong to the *Camarillasaurus* skeleton, having been collected in close proximity to the other elements. This specimen has a well developed concave terminal face (Fig. 3B) and so could be part of a phalanx or a vertebra, but the latter interpretation is most likely because of the structures interpreted as parapophyses. The symmetrical shape of the lateral view (Fig. 3A), with a smooth central channel, a lateral depression, and apparently broken lateral components strongly suggests that this is the floor of a neural canal with broken neural arch elements on either side (Fig. 3B, C). Interpreted as a vertebra, the small size of the specimen is a problem. The fragment is 14 mm long, as preserved, and could have originally been twice that length, say 28–30 mm,

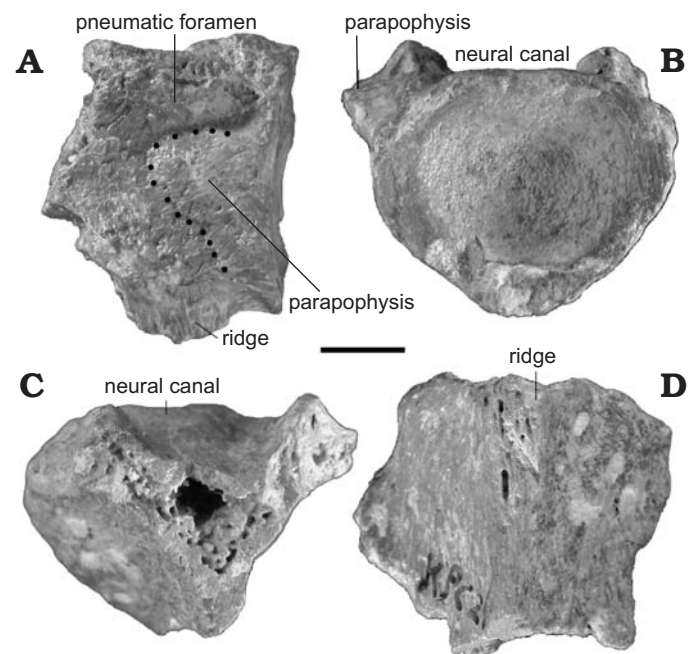


Fig. 3. Ceratosaurian theropod *Camarillasaurus cirugedae* gen. et sp. nov. from the Camarillas Formation of Camarillas, Soria Province, Spain, cervical vertebra, MPG-KPC24, in right lateral (A), ?posterior (B), ?anterior (C), and ventral (D) views. Dotted line in A indicates outline of lateral process (parapophysis). Scale bar 5 mm.

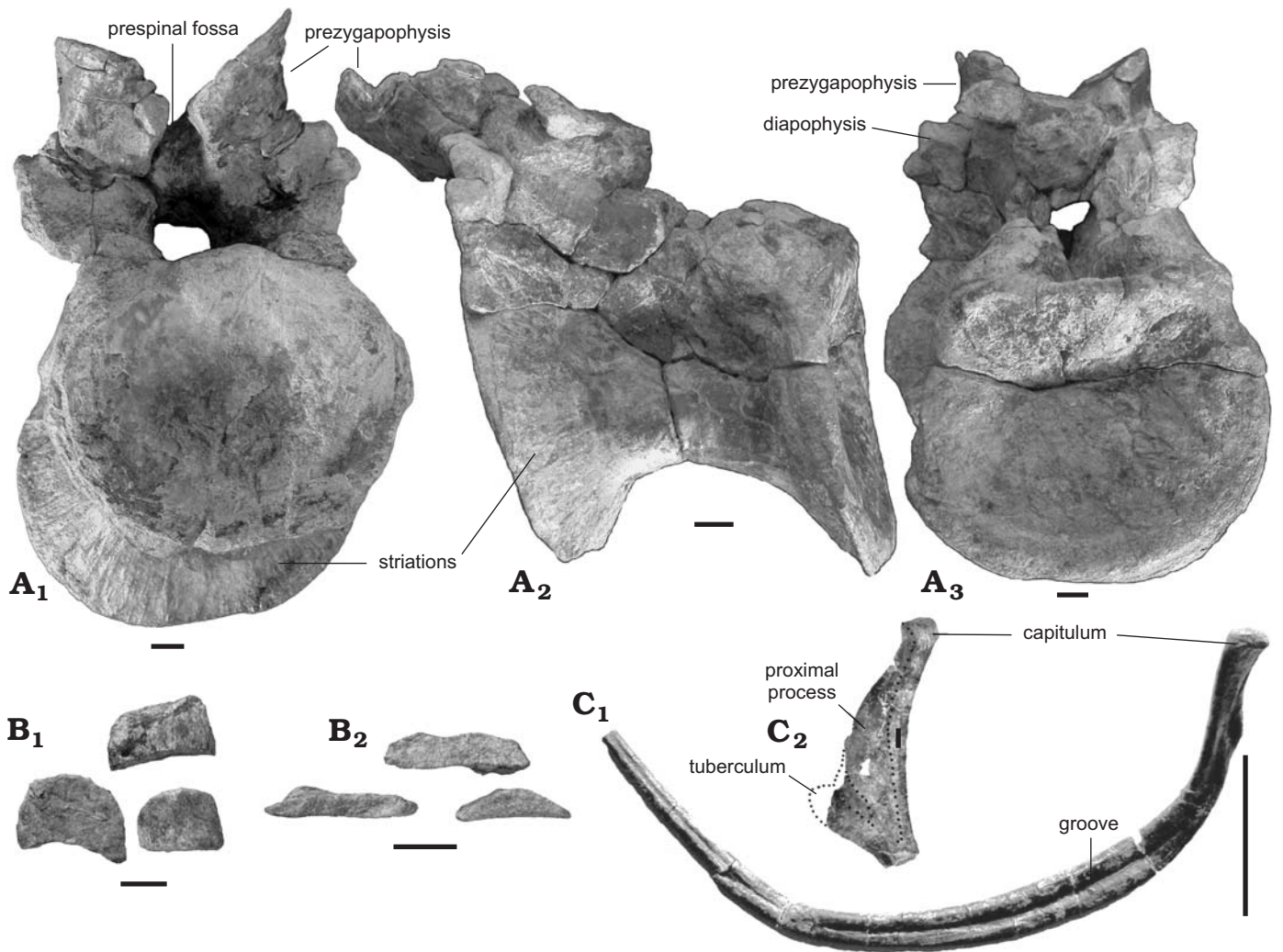


Fig. 4. Ceratosaurian theropod *Camarillasaurus cirugedae* gen. et sp. nov. from the Camarillas Formation of Camarillas, Soria Province, Spain. **A.** Presacral vertebra, MPG-KPC9, in anterior (A_1), left lateral (A_2), and posterior (A_3) views. **B.** Possible neural spine tips, MPG-KPC31, 32, 33, in ?posterior (B_1) and transverse (B_2) views. **C.** Presacral rib MPG-KPC7, in ventral view (C_1) and detail of its proximal end (C_2). Dotted line in C_2 indicates original, restored outline. Scale bars: A , C_2 , 10 mm; B , 20 mm; C_1 , 100 mm.

but this is still half the length expected in proportion to the tooth and to other skeletal elements of *Camarillasaurus*. It is interpreted as an anterior cervical vertebra, and the preserved articular face as the posterior, because it is most similar to the cervical centrum of *Majungasaurus* (O'Connor 2007: fig. 7): both share a concave posterior articular surface that has a straight upper margin, and the centrum has a lateral side with a depression near the top and a projecting structure beneath. In terms of proportions, the *Masiakasaurus* dentary tooth crown length is 6 mm (Carrano et al. 2002: fig. 5) and the length of the cervical vertebra in lateral view is 25 mm (Carrano et al. 2002: fig. 7A), compared to 11 mm and 28 mm respectively in *Camarillasaurus*. We present this possible anterior cervical vertebra only tentatively, because it is small and damaged.

The vertebra lacks one articular face of the centrum and the neural arch is represented only by its base. The putative posterior articular surface (Fig. 3B) is concave and roughly

oval in shape with a slight extension at the base, and it has a dorsoventral height of 12 mm, although the ventral rim is damaged. There is a well developed ventral ridge (Fig. 3A, D). The neural canal (Fig. 3B) is quite wide, becoming narrower towards the midline of the centrum. The lateral surface bears an oval-shaped depression above the parapophysis (Fig. 3A), the pleurocentral depression (O'Connor 2006).

As noted, the fragment matches the concave posterior articular face of the opisthocoelous cervical vertebrae of *Majungasaurus* (O'Connor 2007), and perhaps all or most ceratosaurs had such opisthocoelous cervical vertebrae (a flat anterior face and deeply concave posterior face).

MPG-KPC9 (Fig. 4) is an almost complete vertebra, the largest of all vertebrae from the outcrop. The centrum is spool-shaped in lateral view (Fig. 4A₂), and the anterior face is offset more dorsally than the posterior face as a result of a marked inclination of the centrum. This incline could

be original or partly a result of deformation, but it matches the centrum shape of middle and posterior cervicals of *Majungasaurus* (O'Connor 2007: figs. 8, 9). The articular faces are amphicoelous, oval-shaped, and bear several striations on all the articular surfaces and dorsally (on the centrum, close to the border of the articular surfaces, Fig. 4A₁). There is no evidence of a keel or ridge on the ventral surface. There is a slight depression on the lateral surface (Fig. 4A₂). The neural arch is fused to the centrum, a sign of skeletal maturity, and the prezygapophyses are unfused in the midline. The neural canal is 34 mm high anteriorly, and 39 mm posteriorly. The ratio of anterior centrum height to neural canal height is 3.5.

This vertebra could be a posterior cervical or anterior dorsal, because of the absence of parapophyses on the centrum for contact with the ribs. It is most likely a cervical because the centrum is short, and there is a marked slope in lateral view, with the anterior face located substantially more dorsally than the posterior, similar to the slope seen in middle cervicals of *Majungasaurus* (O'Connor 2007: figs. 8D, 9D).

Dorsal vertebrae.—An almost complete amphicoelous vertebra (MPG-KPC21; Fig. 5C) lacks the anterior articular surface, and is slightly distorted. The centrum is 115 mm long, and the anterior articular face is 109 mm high and 75 mm wide. MPG-KPC21 differs in shape from MPG-KPC9 in having a more ovoid centrum. The centrum is strongly transversely compressed compared to the other vertebrae of *Camarillasaurus*. The centrum does not bear parapophyses on the lateral surfaces. No pneumatic foramen is observed in lateral view, but two shallow elongate depressions are observed on the right lateral side, but are absent on the left. The ventral surface bears a groove between two well developed hypapophyseal ridges. The neural arch is fused, but a great part of it is missing. The parapophysis and postzygapophysis are broken and only the bases can be seen. As in *Ceratosaurus* (Madsen and Welles 2000), the neural canal is oval. The broken base has a maximum width of 20 mm anteriorly, while the maximum width of the postzygapophyses is 17 mm, and they are located 36 mm above the upper surface of the posterior articular face of the centrum. The long axis of the ellipsoidal-shaped articular surface is displaced from the vertical (Fig. 5C₂), presumably by deformation. Based on the proximity between parapophysis and postzygapophysis and the presence of hypapophyses, MPG-KPC21 is identified as an anterior dorsal vertebra. This is further confirmed by the deep groove on the ventral surface which is replaced by a central keel in posterior dorsals, and in the sacral and caudal centra (Coria et al. 2006). It is approximately the fifth dorsal because of its proportions, and by comparison with *Ceratosaurus* (Madsen and Welles 2000) and *Majungasaurus* (O'Connor 2007: fig. 10).

Dorsal vertebrae of ceratosaurs vary substantially in relative length. In MPG-KPC21 the centrum length (in lateral view) is less than 1.1 times the dorsoventral height of the articular surface. This is the same as in *Carnotaurus* (Bonaparte et al. 1990) and *Rajasaurus* (Wilson et al. 2003: fig. 8). This ratio is also less than 1.5 in *Ceratosaurus* (Madsen and

Welles 2000: pls. 7, 17), but at least 2.0 in *Masiakasaurus* presacrals and caudals (Carrano et al. 2011: 21). The presence of shallow pleurocentral depressions (O'Connor 2006), but no apparent pneumatic foramina, differs from the abelisaurid *Kryptops palaios* (Sereno and Brusatte 2008) in which pneumatic foramina are well developed. *Masiakasaurus* loses its pneumatic foramina from the fourth dorsal vertebra (Carrano et al. 2011), and *Ceratosaurus* from the seventh (Madsen and Welles 2000: 17).

A number of further incomplete vertebrae are identified as dorsals. MPG-KPC20 is an isolated half of a transversely compressed vertebra (Fig. 5A). The ventral surface bears a deep ridge. The lateral sides lack pneumatic foramina. The ventral surface of the neural canal and the dorsal margin of the articular surface are flat, not curved. The neural canal width is 1/4 of the dorsoventral height of the articular surface, whereas in MPG-KPC21 this is less than 1/6. Like MPG-KPC20, this is also probably a distal anterior dorsal or proximal mid-dorsal vertebra based on the deep groove on the ventral surface of the centrum.

MPG-KPC17 is a broken posterior centrum, also transversely compressed, but smaller transversely and dorsoventrally, being 2/3 the dorsoventral height of the articular surface of MPG-KPC20 (Fig. 5D). The articular surface is rectangular. Ventrally there is a ridge which joins the deep ventral groove with the ventral edge of the slightly concave articular surface. No pneumatic foramen is observed on the lateral sides. The striations close to the border of the articular surface are not clear, possibly because of damage.

There are two isolated broken neural arches, MPG-KPC51 and 39. MPG-KPC51 is a fragment of the lateral side of a centrum with postzygapophysis (Fig. 5E). Based on its size, it may belong to a posterior cervical vertebra or an anterior dorsal. Three crescent-shaped elements (Fig. 5B₁, B₂) that may be broken tops of neural spines have also been found (MPG-KPC31–33).

MPG-KPC39 (Fig. 5B) is a broken dorsal neural arch. The neural canal is oval-shaped, being wider than tall (14 mm in transverse width, at least 12 mm in dorsoventral height). The prezygapophyses are complete, and the neural spine emerges with a gentle curve, but its length is unknown. Between the prezygapophyses is the prespinal fossa with the dorsoventral longitudinal interspinous ligament scar (Fig. 5B₃), termed the interspinous ligament process (Sereno and Brusatte 2008), or the prespinal and postspinal ridges (Madsen and Welles 2000). Small parts of the centroparapophyseal laminae are preserved and these extend laterally. On the right lateral side (Fig. 5B₂), there are two depressions on the prezygapophyseal surface, placed where Bonaparte et al. (1990: fig. 15B) indicate a pneumatic foramen in the fourth dorsal vertebra of *Carnotaurus*. Nevertheless, unlike *Carnotaurus*, the pleurocentral depression of *Camarillasaurus* is divided in two by a ridge, generating an upper elongate depression and a lower triangular one, a feature not seen in other ceratosaurs (e.g., Carrano et al. 2002, 2011; O'Connor 2007; Sereno and Brusatte 2008). In comparison with other ceratosaur dorsal

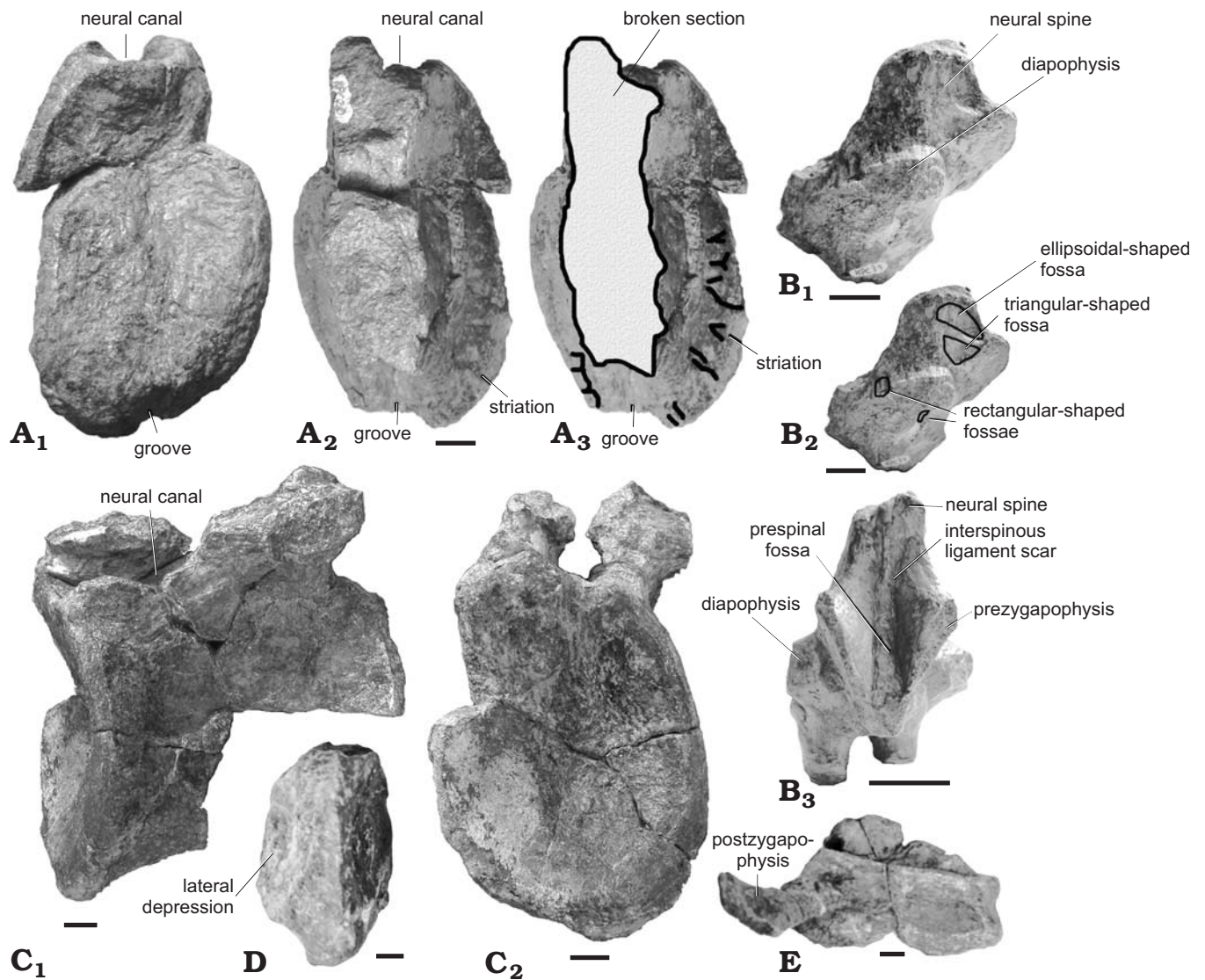


Fig. 5. Ceratosaurian theropod *Camarillasaurus cirugedae* gen. et sp. nov. from the Camarillas Formation of Camarillas, Soria Province, Spain, dorsal vertebrae. A. MPG-KPC20 in ?posterior (A₁) and ?anterior (A₂, A₃) views; showing different structures described in text. B. MPG-KPC39 in right lateral (B₁, B₂), showing structures described in text and in anterior view (B₃). C. MPG-KPC21 in right lateral (C₁) and posterior (C₂) views. D. MPG-KPC17 in left lateral view. E. MPG-KPC51. Scale bars are A, C, D, E, 10 mm; B, 20 mm.

vertebrae, the neural canal is well developed, as in *Ilokelesia* (Coria and Salgado 1998), but it is not so big as in *Masiakasaurus* (Carrano et al. 2002). MPG-KPC39 differs from the unnamed abelisauroid from NW Patagonia (Coria et al. 2006) and the abelisaurid from the Bauru Basin of Brazil (Novas et al. 2008) in lacking the complexity of the laminae. Among other features, MPG-KPC39 differs from the *Kryptops* dorsal vertebra in lacking the deep fossa placed over the neural canal (Sereno and Brusatte 2008). It differs from *Ceratosaurus* (Madsen and Welles 2000), *Kryptops* (Sereno and Brusatte 2008: fig. 6E, F), and *Carnotaurus* (Bonaparte et al. 1990) in the absence of shallow fossae ventrally and below the prezygapophyses. Novas et al. (2008: 631) consider the absence of “anterior infraprezygapophyseal fossae”, which are present in *Ceratosaurus* and basal tetanurans such as *Sinraptor*, *Allosaurus*, and Carcharodontosauridae, as synapomorphic

of Abelisauroidea plus *Spinostropheus*. In *Camarillasaurus* these fossae are absent. The prezygapophyseal facet is longer than in any other ceratosaur, being twice the dorsoventral height of the neural canal. This feature, which could be an autapomorphy of *Camarillasaurus*, is however considered with caution because of damage to the specimen.

Dorsal ribs.—An almost complete presacral rib, MPG-KPC7 (Fig. 4C) is quite curved dorsally, with a strongly convex proximal and a highly concave distal margin. Both lateral sides are flat. There is a longitudinal central broad neurovascular groove (Fig. 4C₁). The blade becomes slender distally and the distal end is missing. The cross section of the shaft is bilobed in the proximal part to oval-shaped in the distal. The rib is approximately five times as long as the anteroposterior length of dorsal vertebra MPG-KPC21 and this length should be greater because of the broken distal pit. The rib has a large

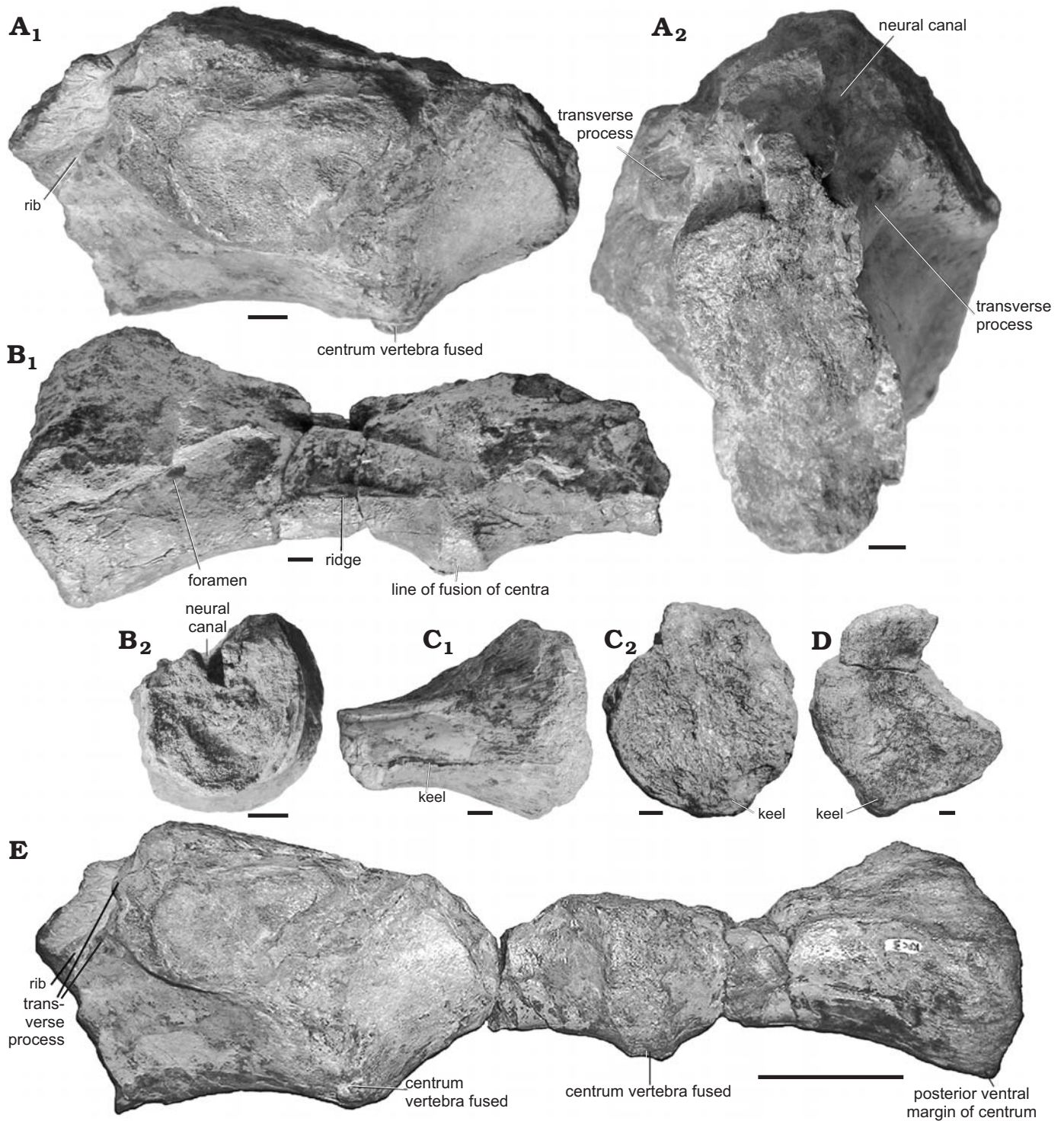


Fig. 6. Ceratosaurian theropod *Camarillasaurus cirugedae* gen. et sp. nov. from the Camarillas Formation of Camarillas, Soria Province, Spain, sacrum. **A.** MPG-KPC4, formed from two broken centra fused, in left lateral (A_1) and anterior (A_2) views. **B.** MPG-KPC3, formed from two broken centra fused, in right lateral (B_1) and anterior (B_2) views. **C.** MPG-KPC16, incomplete centrum, in lateral (C_1) and anterior? (C_2) views. **D.** MPG-KPC18, incomplete centrum, in articular surface ventral view. **E.** MPG-KPC4 and MPG-KPC3, lateral view. Scale bars A–D, 10 mm; E, 40 mm.

capitulum and a robust tuberculum which is wider than the capitulum in cross section, and its proximal part is broken (Fig. 4C₂). Between them there is a large proximal, triangular capitulotubercular concavity which has the proximal rim broken (the proximal process, Fig. 4C₂). Based on the size of

the proximal region, the length of the capitulum blade, and the cross-sectional shape, MPG-KPC7 may be the first or second dorsal rib (cf. *Carnotaurus*; Bonaparte et al. 1990).

Other isolated rib fragments have also been recovered. Some are circular in cross section, similar to that fused with

the sacral centra in MPG-KPC4. Others are bilobed in cross section and considered presacrals for that reason.

Sacral vertebrae.—The sacrum appears to have been formed of six vertebrae, the apomorphic condition for Ceratosauria (Carrano and Sampson 2008). Our specimens include a series of three vertebrae fused together and conserved in two pieces, MPG-KPC4 (Fig. 6A), with two half centra fused, and MPG-KPC3 (Fig. 6B, E), with one and a half fused centra. A further two centra, MPG-KPC16 (Fig. 6C) and 18 (Fig. 6D) are assigned to the sacrum on the basis of shared similarities with the fused centra, such as the ventral surface with one keel, the flat rather than concave articular surface, and the broad border of the articular surface in lateral view. The three fused sacrals (Fig. 6E) are presumably primordial sacral vertebrae 1–3, and these are sacrals 2–4, with 2 and 3 in MPG-KPC4 and 3 and 4 in MPG-KPC3, based on the assumption that at least one dorsal and one caudal vertebra had been recruited into the sacrum, as in *Majungasaurus* (O'Connor 2007).

In MPG-KPC4 and 3, only the centra are preserved, with some portions of the sacral ribs, and the three centra are so extensively co-ossified that the sutures between centra are obliterated. This suggests that the animal had reached adulthood (Tykoski and Rowe 2004). In sequence from front to back, the fused centra become more oval-shaped and lose height and concavity in their articular surfaces. The centra are spool-shaped and the ventral margins are dorsally curved, as is generally the case in ceratosaurians (O'Connor 2007). The three co-ossified vertebrae together form a dorsally convex arch (Fig. 6E), as in *Carnotaurus* (Bonaparte et al. 1990) and *Masiakasaurus* (Carrano et al. 2002), but not as in *Majungasaurus* in which the series forms more of a straight line (O'Connor 2007: fig. 12). The centra are longer than tall, as in *Berberosaurus* (Allain et al. 2007) and *Majungasaurus* (O'Connor 2007), but not as in *Masiakasaurus* in which each sacral vertebra is slightly shorter than tall (Carrano et al. 2002). The centra bear a sharp ventral keel, as in *Allosaurus*, *Ceratosaurus*, Compsognathidae, *Dilophosaurus*, and the abelisaurid *Rajasaurus* (Wilson et al. 2003), but unlike Dromaeosauridae, *Ornitholestes*, Ornithomimosauria, Oviraptorosauria, Therizinosauroida (Rauhut 2003) and the ceratosaurs *Majungasaurus* (O'Connor 2007) and *Masiakasaurus* (Carrano et al. 2011: 20).

The most anterior centrum of MPG-KPC4 (Fig. 6A) recalls the dorsal vertebrae MPG-KPC17, 20, and 21, in being strongly compressed laterally, as in *Carnotaurus* and *Aucasaurus* and the unnamed abelisauroid from NW Patagonia (Bonaparte et al. 1990; Coria et al. 2002, 2006). The most posterior of the three fused sacral centra, in MPG-KPC3, shows the dorsoventrally tallest articular face (Fig. 6B₁, E), similar to the *Carnotaurus* sacrum (Bonaparte et al. 1990: fig. 20C).

In two centra (Fig. 6B₁) there is a longitudinal ridge, rather than pneumatic foramina. The most posterior of the three fused sacral centra, in MPG-KPC3, bears an intervertebral foramen on the lateral face close to the parapophysis (Fig. 6B₁). Pneumatic foramina are also absent in sacrals of *Carnotaurus* (Bonaparte et al. 1990), *Masiakasaurus* (Carrano et

al. 2011), and *Majungasaurus* (O'Connor 2007), but present in Carcharodontosauridae, Maniraptora, Tyrannosauridae, and in many maniraptorans (oviraptorosaurs, many dromaeosaurids, one troodontid) (Benson et al. 2012).

The fused neural arches are broken, but the parapophyses were apparently placed more ventrally than in *Carnotaurus* (Tykoski and Rowe 2004: fig. 3.4A). In MPG-KPC4 there is a proximal portion of a substantial transverse process with a circular cross-section (Fig. 6A). The neural arches are missing, and the base of the neural canal can be seen only in the posteriormost of the fused sacral centra, in MPG-KPC3 (Fig. 6B₁, E).

Two additional broken centra, MPG-KPC16 and 18 (Figs. 6C₁, 7B), may belong to the sacrum based on two features. The exposed articular surfaces are flat rather than concave, as in MPG-KPC3 and 4, and in *Masiakasaurus* (Carrano et al. 2002). Further, both centra have a ventral keel, together with striations on the lateral and ventral sides of the centra, close to the edges of the articular surfaces. It is not possible to say whether these centra lay anterior or posterior to the three fused sacrals (Fig. 6E).

Anterior caudal vertebrae.—Two further half vertebral centra, MPG-KPC14 and 19, may be anterior caudal centra, based on their size and slight concavity of the preserved articular surface. In MPG-KPC14, the edges of this exposed side are broken, showing considerable width of the articular surface. Although the neural arch is lost, its ventral portion is preserved as a dorsal rugosity, showing the transverse width of the neural arch, and possibly also the neural canal. There is no pneumatic foramen. The ventral surface is flat, showing a thin groove.

An isolated half anterior caudal centrum (MPG-KPC19) shares with MPG-KPC14, 16, and 18 some marked striations on the lateral and ventral faces close to the articular surfaces (Fig. 7A). There are two broad, slightly depressed areas on the lateral sides of the centra, but these are not pneumatic foramina as in *Carnotaurus* (Bonaparte et al. 1990). Lateral depressions are also absent in the caudals of other ceratosaurs such as *Ilokelesia* (Coria and Salgado 1998), *Masiakasaurus* (Carrano et al. 2002, 2011), *Ceratosaurus* (Madsen and Welles 2000), and *Rajasaurus* (Wilson et al. 2003). As in MPG-KPC14, the rugosity marking the base of the broken-off neural arch is broad. Only one side of the neural arch has been preserved, showing that the neural canal was considerably reduced (total transverse width of the rugose neural arch base is 59 mm, of which each neural arch pillar measures 25 mm, leaving c. 10 mm for the width of the neural canal). The ventral surface of the centrum does not show a ventral keel, but a midline ridge that demarcates two incipient keels that may mark the site of attachment of a chevron. Comparison with *Carnotaurus* (Bonaparte et al. 1990: fig. 38), suggests this might be the fifth caudal because chevrons occur from this location backwards along the tail.

An isolated broken section of an articular face, MPG-KPC22 (Fig. 7I), could belong to MPG-KPC19. It is a frag-

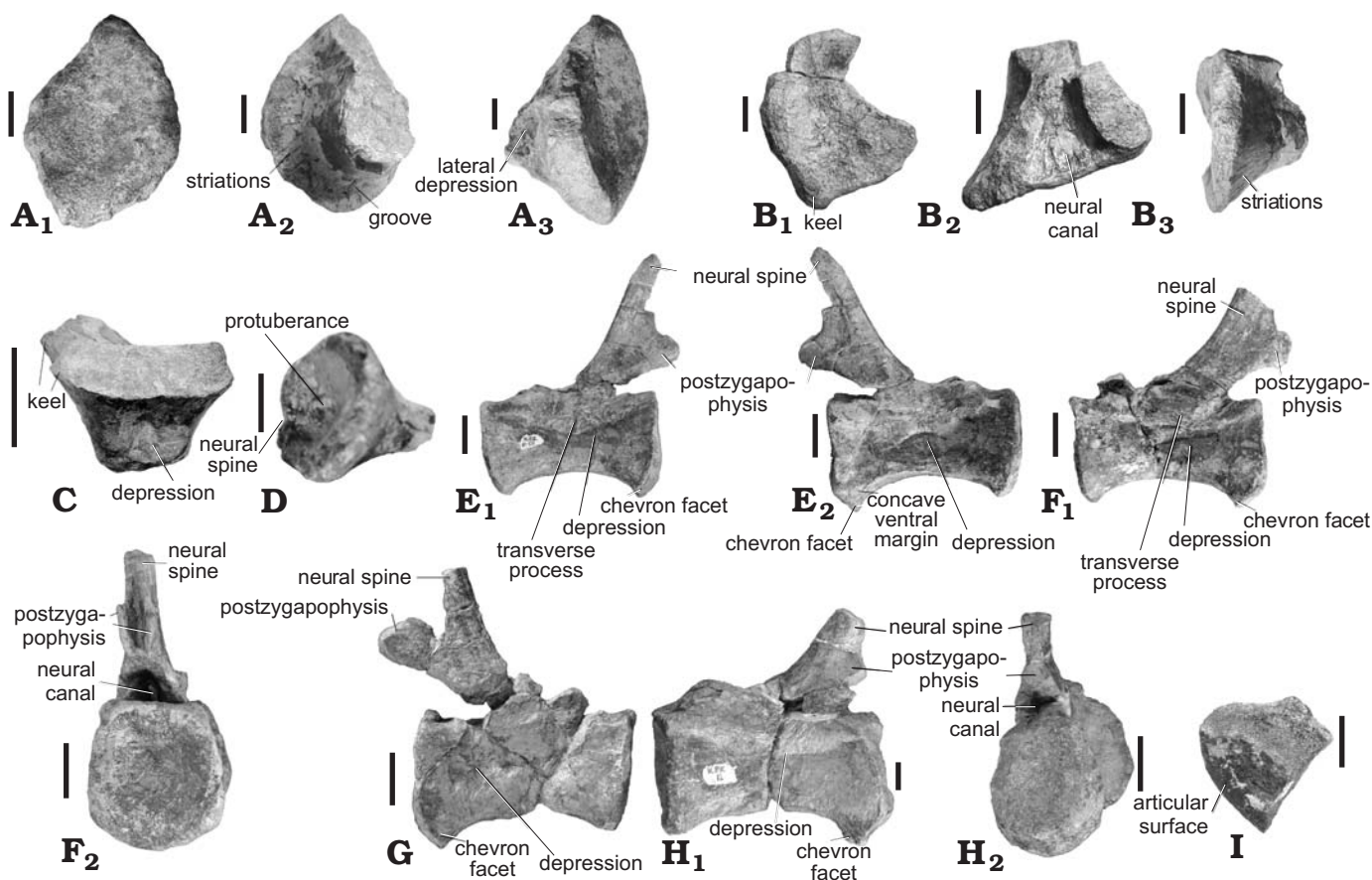


Fig. 7. Ceratosaurian theropod *Camarillasaurus cirugedae* gen. et sp. nov. from the Camarillas Formation of Camarillas, Soria Province, Spain, caudal vertebrae: A. MPG-KPC19, in ?anterior (A₁), ?posterior (A₂), and lateral (A₃) views. B. MPG-KPC18, in ?anterior (B₁), dorsal (B₂), and lateral (B₃) views. C. MPG-KPC15, in lateral view. D. MPG-KPC46, in ?posterior-lateral view. E. MPG-KPC10, in left lateral (E₁) and right lateral (E₂) views. F. MPG-KPC11, in left lateral (F₁) and posterior (F₂) views. G. MPG-KPC13, in left lateral view. H. MPG-KPC12, in left lateral (H₁) and posterior (H₂) views. I. MPG-KPC22, in ?anterior view. Scale bars A₂, C–G, H₂, 20 mm; A₁, H₁, 10 mm.

ment of a concave broken centrum with considerable width near the edge of the broken face.

MPG-KPC15 (Fig. 7C) is another isolated broken caudal centrum that has a pronounced concave articular surface, in contrast with the slightly concave exposed faces of MPG-KPC3, 14, 16, 18, and 19. The margin of the articular surface is broad in lateral view, as seen also in MPG-KPC14 and MPG-KPC15, at least twice the width of this structure in the other *Camarillasaurus* vertebra. The only other feature of MPG-KPC15 are the two well developed keels.

Another isolated broken centrum, MPG-KPC46, has an oval-shaped articular face and a protuberance in the centre of the articular face (Fig. 7D). The ventral surface has no keels or ridges, nor pneumatic foramina. This broken centrum resembles the spool-shaped anterior caudals but is smaller: the dorsoventral height of the articular surface of MPG-KPC16 is 1.4 times that of MPG-KPC46.

Middle and posterior caudal vertebrae.—Four isolated caudal vertebrae, MPG-KPC10–13, have narrow, elongate, spool-shaped centra, and one, MPG-KPC10, also shows most of the neural arch (Fig. 7E). The centra are constricted at mid-centrum length to one-third or one-quarter the width

and height of the articular faces, and the ventral margin is concave. The anterior articular face is somewhat circular and the posterior is elliptical; in other ceratosaurs, the articular faces are either both circular, as in *Carnotaurus* (Bonaparte et al. 1990: fig. 21) and *Masiakasaurus* (Carrano et al. 2002), or both elliptical, as in *Majungasaurus* (O'Connor 2007). Both articular faces are concave, but the posterior face is more deeply concave than the anterior. The anterior and posterior ventral margins show well developed chevron facets, the posterior facet being larger than the anterior, and two keels. There are no pneumatic foramina in the lateral sides. MPG-KPC11 differs from MPG-KPC10, 12, and 13 in having a more marked longitudinal depression where the pneumatic foramen might occur than in the other three vertebrae. MPG-KPC10 and 11 show a well-developed ridge along the side of the centrum, located just below the neurocentral suture, which is presumably the transverse process (Fig. 7E₁, F₁).

In MPG-KPC11, the neural arch is narrow, surrounding a very small neural canal, and the neural spine is tall and slender (Fig. 7F₂). In lateral view (Fig. 7F₁), the neural spine slopes posteriorly, extending beyond the posterior margin of the centrum, and the postzygapophyses are supported by a

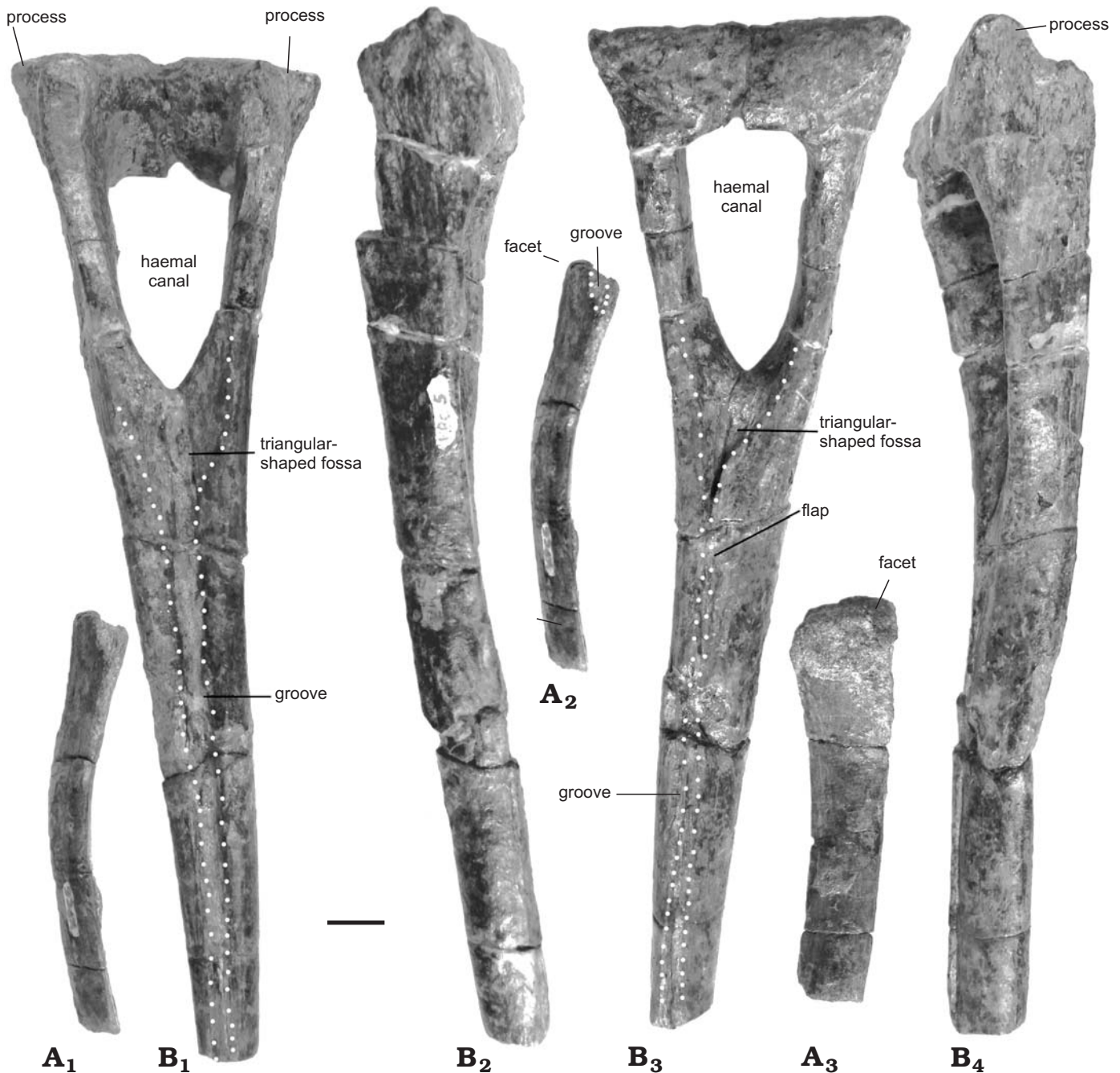


Fig. 8. Chevrons of ceratosaurian theropod *Camarillasaurus cirugedae* gen. et sp. nov. from the Camarillas Formation of Camarillas, Soria Province, Spain. **A.** MPG-KPC6, distal section, in anterior view (A₁), anterior view with different features marked (A₂), left lateral view (A₃). **B.** MPG-KPC5, proximal section with haemal canal, in anterior (B₁), left lateral (B₂), posterior (B₃), and right lateral (B₄) views. Note that the processes are absent on the cranial side. Crests of ridges indicated by white dotted lines in A₂, B₁, B₃. Scale bars 10 mm.

substantial lateral structure beneath the posterior margin of the neural spine. In all four caudals, the preserved part of the neural arch is longer than the height of the corresponding centrum, and wider laterally and anteroposteriorly (Fig. 7). The preserved height of the neural spine is greater than the dorsoventral height of the posterior articular surface of the centrum.

Of the four caudals, MPG-KPC10 and 11 are identified as mid caudals because the centra are less waisted than in anterior caudals and bear well developed transverse process. MPG-KPC12 and 13 are identified as distal caudals because

their centra are slightly longer than in the other two caudal vertebrae, a common feature in theropods (Molnar et al. 1990; Harris 1998), and the concavity of the articular surfaces is greater.

Haemal arches.—An almost complete chevron (MPG-KPC5, 6; Fig. 8) is broad proximally and curves laterally and posteromedially towards the narrow distal end. This chevron is longer than the height of the caudal centra. The proximal end has two anterior projections or knobs that enclose the

haemal canal dorsally. In anterior and posterior views (Fig. 8B₁, B₂), there are longitudinal striations that extend from the proximal projections to the tip of the blade.

The anterior and posterior surfaces have deep midline grooves that reach the distal ends, and the groove is more marked on the anterior than the posterior side (Fig. 8B₁, B₃). A triangular fossa is located below the haemal canal on the anterior and posterior sides arising from the deep groove. On the posterior side, below the triangular fossa, the longitudinal groove is covered by a thin bone lamina (Fig. 8B₃). The distal end of the chevron (MPG-KPC6; Fig. 8A) is expanded and is wider laterally than posteriorly, and it bears a distal facet (Fig. 8A₂, A₃). This facet may indicate that the distal tip was in contact with another chevron blade, suggesting that the chevrons were long and overlapping, and set at an acute angle to the caudal vertebral column (Bonaparte et al. 1990: 21).

MPG-KPC44 is an isolated broken blade of a chevron, again with a deep groove along the blade. Based on the preserved length, it probably attached to an anterior or middle caudal centrum.

The *Camarillasaurus* chevron recalls that of *Ilokelesia* (Coria et al. 2006) and *Majungasaurus* (O'Connor 2007: fig. 19) in general morphology. However, the deep groove along the length of the haemal spine is unlike *Ilokelesia*, *Carnotaurus*, and *Majungasaurus* in which the groove is restricted to the proximal part (Bonaparte et al. 1990; Coria and Salgado 1998; O'Connor 2007). Further, the *Ilokelesia* and *Majungasaurus* chevrons do not have an expanded distal end (Coria and Salgado 1998; O'Connor 2007), although this is seen in *Masiakasaurus* (Carrano et al. 2011: 23). The anterior edge of the proximal surface in MPG-KPC5 is located more ventrally than the posterior edge, whereas in *Ceratosaurus* both edges are at the same level. *Camarillasaurus* differs from *Ilokelesia*, *Masiakasaurus* and *Carnotaurus* in having a quite developed haemal canal that occupies a third of the total length of the chevron and in the presence of a triangular fossa below the haemal canal. These fossae are also absent in *Ceratosaurus* chevrons (Madsen and Welles 2000).

Appendicular skeleton

Pectoral girdle.—An incomplete right pectoral girdle (MPG-KPC23, 30; Fig. 9) is the only preserved element of the forelimb skeleton. It consists of the incomplete right scapulocoracoid, a section of the scapular blade, and the right sternal plate MPG-KPC2. Of the left pectoral girdle, only the left sternal plate is known.

The partial right scapular blade MPG-KPC30 (Fig. 9B₁) is flat and roughly straight-sided, 170 mm long, 66 mm wide, and 28 mm thick. The specimen is incomplete, but the scapula was presumably long and had an unexpanded distal end, by comparison with other ceratosaur scapulae (Tykoski and Rowe 2004). In lateral view, the blade is flat, whereas in medial view it is convex more markedly towards the distal end of the blade, close to the anterior rim, which is thinner than the posterior edge (Fig. 9B₁, B₂). On the lateral surface, close to the anterior edge, and marked by a broad white arrow in

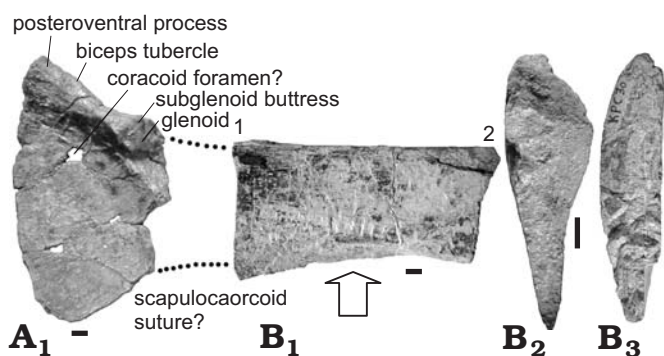


Fig. 9. Broken right scapulocoracoid of ceratosaurian theropod *Camarillasaurus cirugedae* nov. gen. et sp. from the Camarillas Formation of Camarillas, Soria Province, Spain. **A.** MPG-KPC23, in medial view. **B.** MPG-KPC30, in medial (B₁), posterior (B₂), and anterior (B₃) views (sections at lines “1” and “2” respectively). An arrow points to ridges that might indicate a muscle insertion, or tooth marks. Scale bars 10 mm.

Fig. 9B, there is a striated region that could indicate a muscle insertion, although the six parallel depressions are rather well defined, and recall the tooth marks noted in *Majungasaurus* (Rogers et al. 2003: fig. 1C).

The right coracoid MPG-KPC23 (Fig. 9A) may also retain part of the base of the conjoined scapula. The posterior margin supports a broad glenoid facet, and there is a faint suture running anterior to the glenoid that might mark the division between the two bones. This is unclear, as is the possible coracoid foramen, because the specimen was already broken into several fragments when it was collected. The preserved coracoid is 187 mm long. The ventral margin forms an angle of 55° with the anterior margin, and 45° with the posterior margin. The ventral margin is unusual in being only slightly convex ventrally, so that the coracoid is more rectangular than semicircular. In medial view, the ventral margin is more or less straight, as in *Carnotaurus* (Bonaparte et al. 1990: fig. 27B), *Majungasaurus* (Carrano 2007: fig. 2) and *Coelophysis* (Harris and Downs 2002: fig. 3D). The coracoid is a thin plate anteriorly and it thickens to a posterior pillar below the glenoid. The subglenoid buttress (Madsen and Welles 2000: pl. 20A) is preserved below the glenoid. On the posterior edge of the coracoid, above the subglenoid ridge, the biceps tubercle (Madsen and Welles 2000: pl. 20A) is preserved as a slight protuberance. The acromion area is missing. In other ceratosaur coracoids (Bonaparte et al. 1990; Madsen and Welles 2000; Harris and Downs 2002; Tykoski and Rowe 2004; Carrano 2007), below the glenoid there is a rounded posteroventral process. The coracoid of *Camarillasaurus* is unique, however, in the combination of a subglenoid ridge that arises from the glenoid and has a nearly straight abrupt border finishing in a tapering process. The posteroventral process is not so extensive as in *Carnotaurus* and it is not placed so horizontally, nor so vertically as in *Ceratosaurus*, but it is more similar to the *Majungasaurus* scapulocoracoid FMNH PR 2278 (Carrano 2007) than FMNH PR 2836 (Burch and Carrano 2012) which has a prominent rounded posteroventral process. These two taxa differ in the glenoid lips observed

in *Majungasaurus* and the glenoid ridge of *Camarillasaurus* which seems to be absent in *Majungasaurus* (Carrano 2007; Burch and Carrano 2012), but also in other ceratosaurs such as *Ceratosaurus*, *Carnotaurus*, and *Elaphrosaurus* (Tykoski and Rowe 2004). The scapulocoracoid of *Camarillasaurus* is S-shaped in lateral and medial views, as in *Ceratosaurus* (Madsen and Welles 2000) and *Dilophosaurus* (Tykoski and Rowe 2004), but unlike in *Carnotaurus* (Bonaparte et al. 1990), *Syntarsus* (Tykoski and Rowe 2004) and *Majungasaurus* (Carrano 2007, Burch and Carrano 2012).

There are two complete sternal plates (MPG-KPC1, 2) and some sternal fragments (MPG-KPC34–38). MPG-KPC1 (Fig. 10A), the left sternal plate, is triangular in shape, curved posteriorly, and about 230 mm long and up to 145 mm wide. MPG-KPC2 (Fig. 10B), the right sternal plate, is lanceolate-shaped with a height of 228 mm and a maximum lateral-ventral width of 122 mm. Both plates are about 10 mm thick. On the lateral and ventral side there is a thin carina. The lateral surfaces are vascularized, and towards the top there are vertical grooves that are narrower than on the rest of the surfaces. There is a deep groove, the coracoid sulcus (Fig. 10A₁, B₁), and the attachment mark of a sternal rib (Fig. 10A₂) on the lateral face of MPG-KPC2. The differences in morphology between these two sternal plates could arise from damage suffered by MPG-KPC2.

Preserved sternal plates are very rare in theropods, suggesting either that they are absent or at least not found or reported, in most taxa. However, we argue that these specimens cannot be either scapular fragments or iliac plates. MPG-KPC1 and 2 differ from the incomplete right scapulocoracoid (MPG-KPC23, 30; Fig. 9) in their size (being larger), curvature (the dermal plates are flat and thinner than the curved scapulocoracoid), and ornamentation (the surfaces of the sternal plates are vascularized while those of the scapulocoracoid are not). Further, neither could be considered as an ilium because of the absence of typical iliac structures. This is only the second time that sternal plates have been described in a ceratosaur, after *Carnotaurus* (Bonaparte et al. 1990). Their absence in other ceratosaurs may be a result of non-fossilisation or non-collection rather than absence.

Tibia.—The proximal end of a right tibia, MPG-KPC8 (Fig. 11), has a total preserved length of 293 mm. The proximal end measures 180 by 64 mm, giving it the highest ratio of maximum: minimum proximal tibial diameter for any theropod (Table 1). The anterior margin of the tibia is slightly curved, the posterior margin more straight. The anterior curve to the cnemial crest is less marked than in *Masiakasaurus* (Carrano et al. 2002: fig. 15G) and *Majungasaurus* (Carrano 2007: fig. 6A). Because of the straight posterior margin and the absence of curvature, the lateral fossa is also less marked than in *Masiakasaurus*. The cross section of the tibial shaft is oval, broadest anteroposteriorly. Most of the original bone surface is preserved, although the cnemial crest area is damaged, in the anteriormost portion and at the distal end.

In lateral view (Fig. 11A), the cnemial crest is greatly expanded, and rises proximally higher than the lateral and

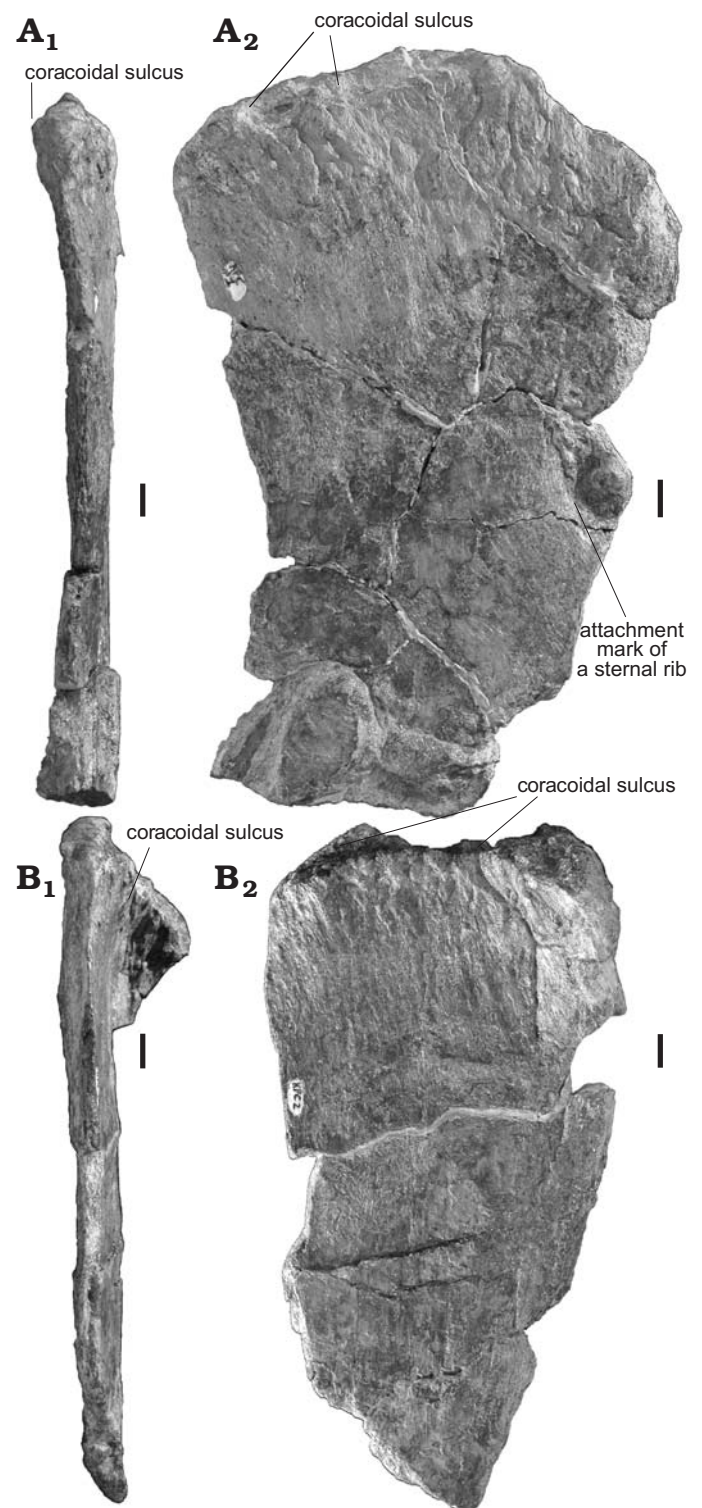


Fig. 10. Sternal plates of ceratosaurian theropod *Camarillasaurus cirugedae* gen. et sp. nov. from the Camarillas Formation of Camarillas, Soria Province, Spain. A. MPG-KPC2, right sternal plate, in lateral (A₁) and ventral (A₂) views. B. MPG-KPC1, left sternal plate, in lateral (B₁) and ventral (B₂) views. Scale bars are 10 mm.

medial condyles. It is flanked laterally by the fibular crest which runs the length of the specimen (Fig. 11B–D). As the cnemial and fibular crests approach each other distally, they

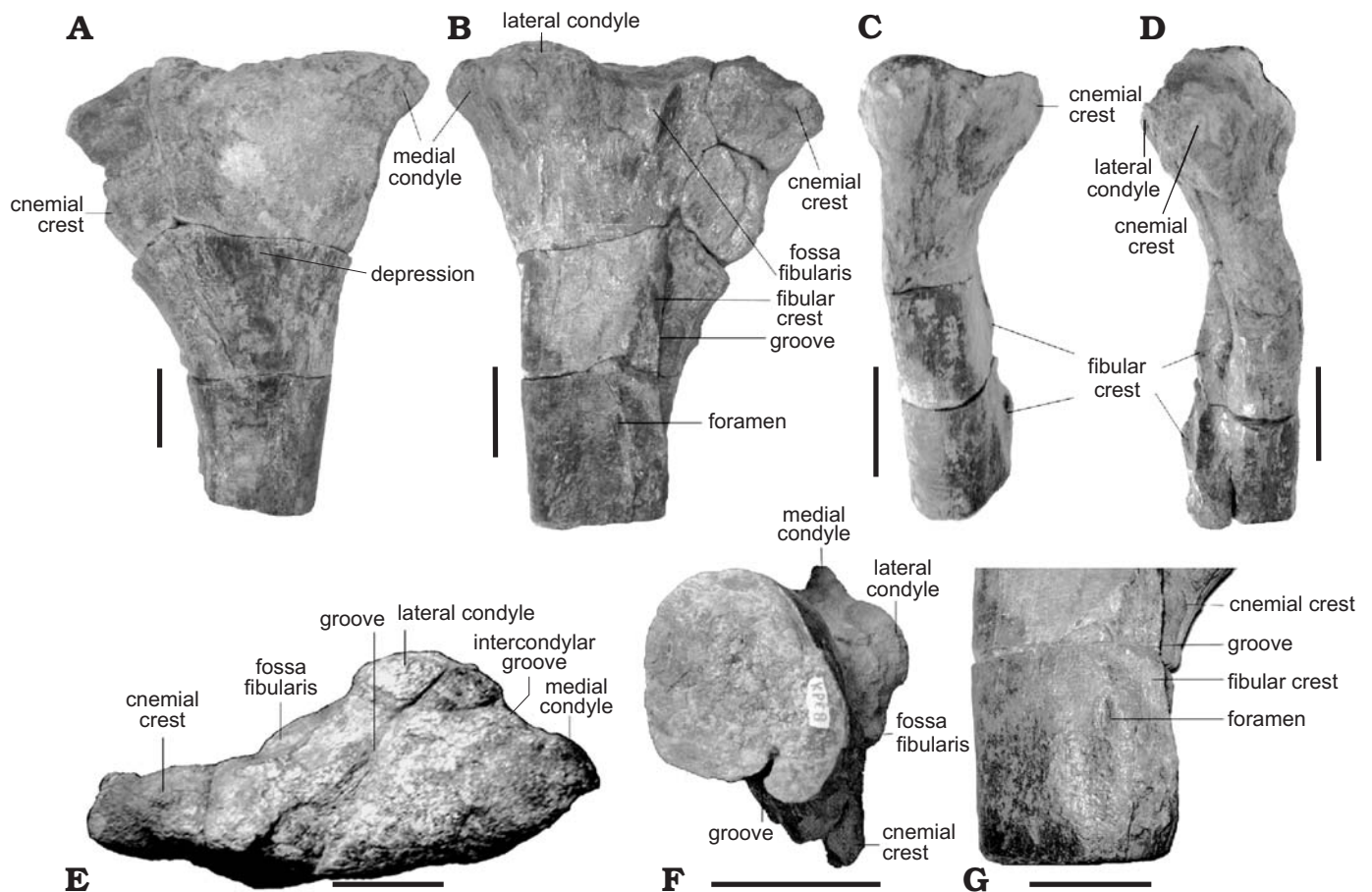


Fig. 11. Proximal portion of right tibia of ceratosaurian theropod *Camarillasaurus cirugedae* nov. gen. et sp. from the Camarillas Formation of Camarillas, Soria Province, Spain, MPG-KPC8, in lateral (A), medial (B), anterior (C), posterior (D), proximal (E), and distal (F) views; detail of the tibial foramen area, in lateral view (G). Scale bars 10 mm.

generate a longitudinal groove or fossa (Fig. 11B; lateral fossa of Carrano 2007: fig. 6), which continues down the fibular crest as a deepening groove. In the distal broken shaft section (Fig. 11F), the longitudinal groove is seen in cross section as a smooth-walled notch, giving the tibial shaft a distinct g-shaped cross section (Fig. 11F). The great extent of this lateral fossa in *Camarillasaurus* seems to be unique. At the distal end of this groove, and offset to the side, is a large nutrient foramen (Fig. 11B, G). In the area of the fossa, foramen and fibular crest (Fig. 11B, G), the bone is not damaged, and it shows the same smooth brown surface as elsewhere (the broken areas have a grey coloration) and the longitudinal groove and fossa are smooth-margined and so are not breaks or other damage.

The proximal articular face of the tibia (Fig. 11E) is concave and rugose and a narrow groove runs diagonally from the middle of the lateral condyle to the middle of the medial margin. The proximal end is mediolaterally broad, extending from the somewhat squared laterally placed cnemial crest to the angular medial condyle. The lateral condyle is well developed and, as in *Majungasaurus* (Carrano 2007) in lateral view the posterior edge of the tibia is angled obliquely relative to the mediolateral axis. Between the lateral and medial condyles there is an intercondylar groove rather than

the intercondylar notch observed in other theropods. This groove runs from the intercondylar area and medially directed in proximal view to the proximal articular surface (Fig. 11C, E). Between lateral condyle and cnemial crest is the broad, concave fossa fibularis. The fibular crest, located centrally in the fossa fibularis (= lateral fossa), does not contact the triangular “cranio-lateral projection” of the fossa fibularis (Naish 2003: figs. 4, 5) on the proximal surface. The proximal end of the tibia is similar in shape to *Xenotarsosaurus*, *Masiakasaurus* (Carrano et al. 2002), and *Ceratosaurus* sp. from the Upper Jurassic of Portugal (Antunes and Mateus 2003), but the latter lacks the tibial foramen seen in the *Camarillasaurus* (Octavio Mateus, personal communication 2012).

The prominence of the cnemial crest, rising proximally higher than the lateral and medial condyles, is typical of most tetanurans (e.g., *Neovenator*, Brusatte et al. 2008: fig. 22; *Megalosaurus*, Benson 2010: fig. 17), but unusual for a ceratosaur: in most ceratosaur, for example *Majungasaurus* (Carrano 2007), *Carnotaurus* (Bonaparte et al. 1990), *Aucasaurus* (Coria et al. 2002), and *Quilmesaurus* (Juárez Valieri et al. 2007), the cnemial crest is more prominent.

The fossa fibularis, quite well developed in other theropod tibiae, is only slightly marked here, and it is lateral-

Table 1. Ratio of minimum to maximum diameter of the proximal end of the tibia for a number of theropods. Measurements with an asterisk (*) are estimated from illustrations; the others are taken from cited measurements. Measurements are in mm. Abbreviations: AP, antero-posterior diameter; ML, mediolateral diameter.

Taxon	ML	AP	Ratio	Source
Ceratosauria				
<i>Camarillasaurus</i>	180	64	2.8	original data
<i>Xenotarsosaurus</i> *	340	180	1.9	Bonaparte (1991)
<i>Carnotaurus</i> *	250	140	1.8	Bonaparte et al. (1990)
<i>Masaiakasaurus</i> 1	175	107	1.6	Carrano et al. (2002)
<i>Majungasaurus</i>	702	552	1.3	Carrano (2007)
<i>Masaiakasaurus</i> 2	166	138	1.2	Carrano et al. (2002)
<i>Elaphrosaurus</i>	120	90	1.3	Tykoski and Rowe (2004)
Tetanurae				
<i>Neovenator</i>	225	117	1.9	Brusatte et al. (2008)
Allosauroid	180	100	1.8	Naish (2003)
Coelurosaurier A	17	30	1.8	Rauhut (2005a)
Coelurosaurier C	25	46	1.8	Rauhut (2005a)
<i>Deinonychus</i>	74	44.8	1.7	Ostrom (1969)
<i>Allosaurus</i> *	210	145	1.5	Madsen (1976)
<i>Megalosaurus</i> *	220	155	1.4	Benson (2010)
<i>Sinraptor</i> *	350	260	1.3	Currie and Zhao (1993)
Basal				
<i>Dilophosaurus</i>	145	80	1.8	Welles (1984)

ly occupied by the craniolateral projection (Fig. 11), as in *Majungasaurus* (Carrano 2007: fig. 6A). Nevertheless, this structure is not as close to the lateral condyle as in *Majungasaurus*, only separated by a notch (Carrano 2007: fig. 6). Also as in *Majungasaurus*, the intercondylar notch is represented by a groove that runs from the intercondylar area and is medially directed in proximal view to the proximal articular surface (Fig. 11C, E), as in Carcharodontosauridae (Serenó 1999), the coelurosaur *Tugulusaurus* (Rauhut and Xu 2005) and the ceratosaurian *Masiakasaurus* (Rauhut 2005a). This groove is also present in the medial condyle of *Majungasaurus*.

The well developed lateral fossa of the cnemial crest in *Camarillasaurus* is quite different from the slightly developed fossa in *Indosuchus* (Juárez Valieri et al. 2007), *Genusaurus*, *Aucasaurus*, *Quilmesaurus* (Juárez Valieri et al. 2007), *Ceratosaurus* (Madsen and Welles 2000), *Majungasaurus* (Carrano 2007), and its total absence in *Ekrixinatosaurus* and *Berberosaurus* (Juárez Valieri et al. 2007). *Carnotaurus* and *Xenotarsosaurus* seem to have a lateral fossa behind the cnemial crest, more like *Camarillasaurus* than the other ceratosaur genera mentioned. *Limusaurus* (Xu et al. 2009) has a lateral fossa that appears to be as well developed as in *Camarillasaurus*. It also appears to have a nutrient foramen located at the midline of the cnemial crest length, more anteriorly than in MPG-KPC8. The unnamed abelisauroid from Libya (Smith et al. 2010) shows an intermediate condition of the lateral fossa, between that of *Carnotaurus* and *Xenotarsosaurus* on the one hand, and the well developed structure of *Camarillasaurus* and *Limusau-*

rus. The isolated Libyan tibia differs in the lateral condyle, which is less developed than in *Camarillasaurus*, and the absence of the lateral groove on the lateral fossa observed in *Camarillasaurus* and *Limusaurus*. The nutrient foramen is present in nearly all theropods.

Remarks

Generic identity.—*Camarillasaurus* differs from all named theropods in possessing at least three autapomorphies: (i) the ratio of minimum to maximum diameter of the proximal end of the tibia is very high, measuring 2.8; (ii) g-shaped cross-section of the shaft of the tibia produced by the central narrow deep longitudinal groove on the medial surface, placed anteriorly to the fibular crest; (iii) chevron with a deep longitudinal groove along the length of the shaft on the anterior and posterior sides. A possible fourth apomorphy is the large, rounded sternal plates, but they are incomplete and their shape cannot be confirmed conclusively.

Of basal ceratosaurs, *Ceratosaurus* differs from *Camarillasaurus* in having a dorsoventrally narrower coracoid (Tykoski and Rowe 2004), and a not so marked difference between the first sacral centra and the last ones (Molnar et al. 1990). *Elaphrosaurus* differs in having a length/width ratio of the proximal tibia lower than in *Camarillasaurus* (Table 1). From *Carnotaurus*, the new Spanish theropod differs in the curved scapular blade, the sharp longitudinal groove on the proximal posterior ventral surface (Bonaparte et al. 1990), the sacral transverse processes (Tykoski and Rowe 2004), and the deep groove along the chevron shaft. Although *Majungasaurus* has a flat area adjacent to the carinae, as in *Genyodectes*, both genera show teeth laterally wider than in *Camarillasaurus* (Rauhut 2004). The posterodistal process of the coracoid of *Camarillasaurus* differs from all other ceratosaur genera.

Of Late Cretaceous abelisauroids, *Xenotarsosaurus* has a narrower proximal tibial shaft (Martínez et al. 1986) than in the new Spanish theropod. *Camarillasaurus* differs from *Masiakasaurus* in the broad morphology of the teeth in lateral view (strongly compressed labiolingually in *Masiakasaurus*), the midsacral centra being more reduced in size, and in a sacral ventral margin more curved than in *Masiakasaurus* (Carrano et al. 2002; Wilson et al. 2003; Tykoski and Rowe 2004). Further, the lateral fossa in the *Camarillasaurus* tibia is also less marked than in *Masiakasaurus* (Carrano et al. 2002).

The tibia of *Velocisaurus* (Mateus et al. 2006) and the unnamed Libyan abelisauroid (Smith et al. 2010) is more gracile than in *Camarillasaurus*. The haemal canal in the *Camarillasaurus* chevron is larger than in *Ilokelesia*, but unlike in *Aucasaurus*, it is dorsally closed. The triangular-shaped fossa behind the haemal canal observed in the cranial and caudal sides of *Camarillasaurus* chevrons may be present on one side in other ceratosaurs, but never in both. The lateral condyle proximally placed are further differences from *Aucasaurus* (Coria et al. 2002). *Camarillasaurus* differs from *Rajasaurus* in the sacrum, slightly curved

dorsally in the former (Wilson et al. 2003), and in having two ventral keels on the anterior caudal centra and not one. Compared to *Majungasaurus*, *Camarillasaurus* lacks the particular morphology of the proximal part of the tibia, and the slender caudal centrum (Tykoski and Rowe 2004; Krause et al. 2007). *Limusaurus* (Xu et al. 2009) differs from *Camarillasaurus* in its slender tibia and in the coracoid morphology (subrectangular-shaped for *Camarillasaurus*, semicircular-shaped for *Limusaurus*).

Phylogenetic affinities.—*Camarillasaurus* does not show the synapomorphies of Saurischia listed by Rauhut (2003) and Langer and Benton (2006) because these are features of the skull, mandible, presacral neural arch, hand, and ischium. The same is true for synapomorphies of Theropoda listed by Rauhut (2003), except for the distal end of the chevron (MPG-KPC5, 6; Fig. 8), which lacks the theropod character of an anteriorly directed process. Nevertheless, *Camarillasaurus* shares the theropod synapomorphies of five sacral vertebrae (at least six have been preserved), fibula closely appressed to the tibia and attached to a tibial crest, and thin-walled, hollow long bones (Gauthier 1986).

Camarillasaurus is a member of Neotheropoda based on the presence of at least five sacral vertebrae and a ventral groove in the anterior caudals (Rauhut 2003; Carrano et al. 2012). The tibia shows a ridge on the proximal end of the lateral side of the tibia for attachment of the fibula, but lacks the neotheropod cleft between the medial side of the proximal end of the tibia and fibular condyle posteriorly (Rauhut 2003), although this is reversed also in *Bagaraatan* and *Avimimus*. It is not possible to identify characters in our material that match further nodes between Neotheropoda and Ceratosauria in Rauhut’s (2003) or Carrano and Sampson’s (2008) analyses.

Within Averostra (Ceratosauria + Tetanurae), it cannot be determined whether *Camarillasaurus* is a tetanuran or not as it lacks relevant elements (skull, humerus, hand, ischium, foot). It also lacks the ilium and femur, so it cannot be determined whether the Spanish animal belongs to Orionides (Carrano et al. 2012). Of major clades within Tetanurae, likewise, *Camarillasaurus* cannot be assessed as a member of Megalosauroidea as it lacks the skull, and of Allosauroidea as it lacks the skull, humerus, metatarsals, and appropriate features of dorsal vertebrae and chevrons. Carrano et al. (2012) note two characters for Coelurosauria, posteriormost dorsal vertebrae with parapophyses distinctly below the transverse process, which cannot be assessed in *Camarillasaurus*, and a tapering distal end in anterior and middle chevrons, which is present.

More convincing, however, is the evidence that *Camarillasaurus* is a ceratosaur. It possesses sacral centra fused to an extreme degree, where the sutures are difficult to discern and only swell around the articular surfaces of the centrum (Tykoski and Rowe 2004: 57). In addition, it shows a sharp ventral groove (double ventral keels) on at least the proximal caudal centra (Tykoski and Rowe 2004), an apomorphy of Ceratosauria, but seen also in the tetanurans *Sinraptor*

(Currie and Zhao 1993) and *Piatnitzkysaurus* (Carrano et al. 2012). Of the 15 synapomorphies of Ceratosauria identified by Carrano and Sampson (2008: 201), *Camarillasaurus* does appear to have had six sacral vertebrae (character 93[2]), although it cannot be said for sure whether the mid-sacral centra were more laterally compressed or not (character 94). Characters of the sacral neural spines (characters 96, 98) cannot be assessed. The dorsoventral depth of the coracoid is more than half its anteroposterior length, although not so deep as in some other ceratosaur (character 108). The other ceratosaur apomorphies (Carrano and Sampson 2008; characters 72, 73, 90, 110, 111, 113, 118, 128, 138, 141) cannot be assessed, either because the material is incomplete (presacral pneumaticity, projecting transverse processes) or we lack appropriate elements (humerus, ilium, ischium, fibula, astragalus).

According to Carrano and Sampson (2008), Ceratosauria comprises *Elaphrosaurus* and its relatives as the most basal ceratosaur, followed by *Ceratosaurus* and Noasauridae + Abelisauridae (= Abelisauroidae). Several additional forms were identified as noasaurids, including *Genusaurus*. Within Abelisauridae, their analysis reveals a clade including *Majungasaurus* and the Indian forms, as well as a more weakly supported clade comprising *Carnotaurus* and *Ilokelesia*.

Phylogenetic analysis.—The relationships of *Camarillasaurus* are assessed by means of a phylogenetic analysis founded on the data matrix in Carrano and Sampson (2008), who provide the most recent comprehensive phylogenetic study of Ceratosauria. We first re-ran the analysis using PAUP* 4.0b10 (Swofford 2002), with all characters equally weighted, and all unordered, except character 141 which was ordered, and with all settings as in the original analysis, and we replicated the results of Carrano and Sampson (2008).

We then added two taxa, *Camarillasaurus* and *Limusaurus*, coded for the 151 characters in Carrano and Sampson (2008), as listed in Table 2. *Limusaurus* was determined as a basal ceratosaur by Xu et al. (2009), but has not previously been included in this data matrix. We ran our analysis with equally weighted parsimony using TNT v. 1.0 (Goloboff et al. 2008). We first ran the “Traditional” search option (5000 replicates, tree bisection and reconnection), and then using the “New Technology” search option to find all tree islands

Table 2. Coding of the 151 characters from Carrano and Sampson (2008) for *Camarillasaurus* and *Limusaurus*. [N – inapplicable because refers to teeth].

<i>Camarillasaurus</i>	???? ???? ???? ???? ???? ???? ???? ???? ????? ????? ????? ????? ????? ????? ?0??? ????? 0???? ????? ?1111 011?0 0???1 101?? ????? ????? ????? ????? ????1 ????? ????? ?
<i>Limusaurus</i>	001?1 1???0 00000 01000 00000 000?0 ?0000 ?0?00 ????? ????? ????? ?1N0 ?1?0 0NN?? ?00?? ?02?1 1???? 0???0 ????? ????0 ?0101 00010 ?1101 01101 11?11 1?100 ?12?1 1?1?? ?1?? 1101? 1

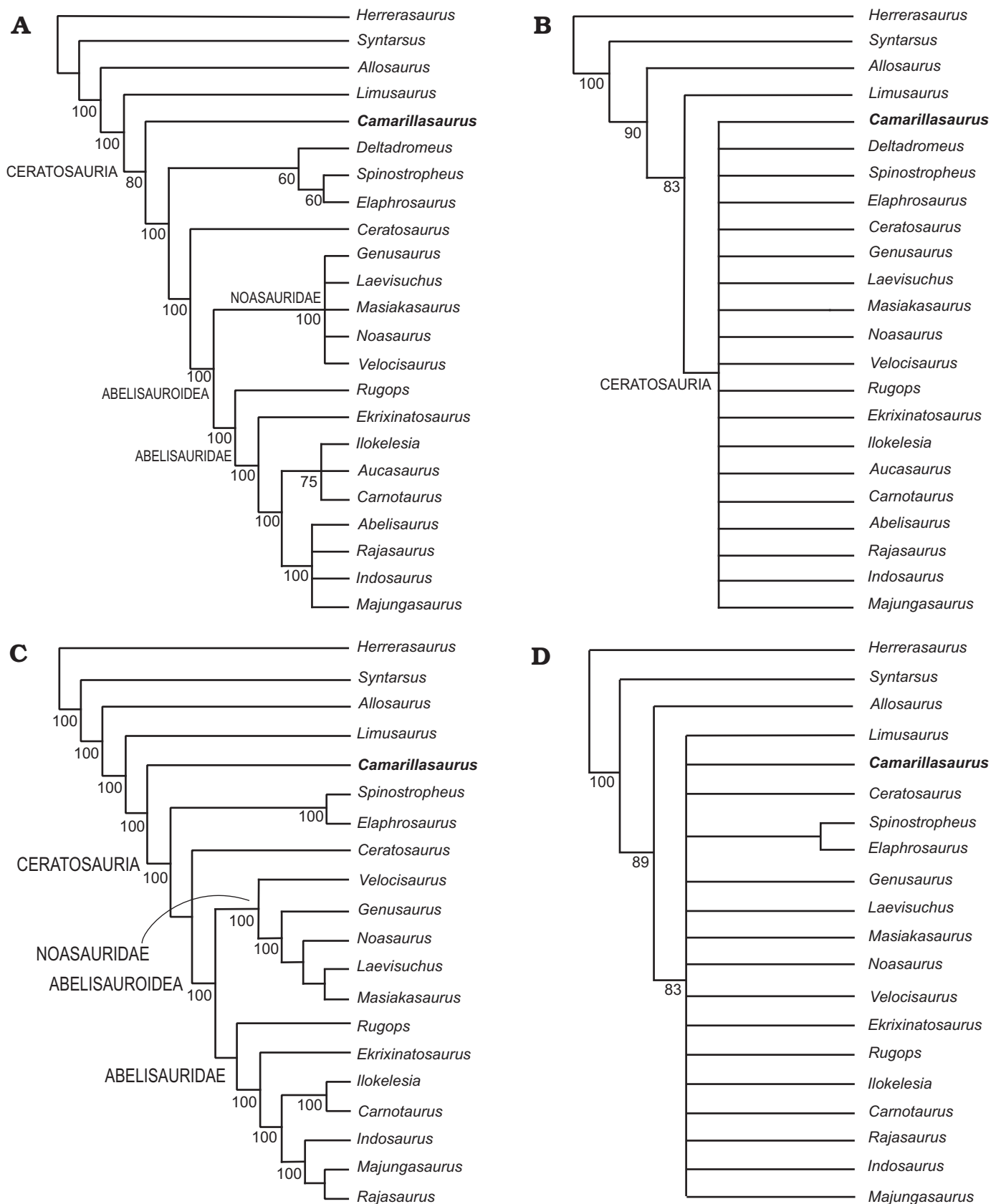


Fig. 12. Phylogenetic position of *Camarillasaurus cirugedae* gen. et sp. nov. among other Theropoda. **A, B.** Re-run of the Carrano and Sampson (2008) cladistic analysis, with addition of *Limusaurus* and *Camarillasaurus*, showing the 50% majority-rule tree (**A**) and strict consensus tree with bootstrap values over 50% (**B**). **C, D.** Re-run of the Carrano and Sampson (2008) cladistic analysis, with three taxa (*Deltadromeus*, *Aucasaurus*, *Abelisaurus*) pruned and with addition of *Limusaurus* and *Camarillasaurus*, showing the sole most parsimonious tree (**C**) and strict consensus tree with bootstrap values over 50% (**D**).

(sectorial search, ratchet, and tree-fusing search methods, all with default parameters). To assess tree robustness, 1000 bootstrap replicates were run in TNT, and nodes with bootstrap values <50% were collapsed.

In the re-run of the Carrano and Sampson (2008) analysis, we recovered 10,560 trees of length 241 steps, longer than found in the original analysis (10,560 trees of length 220 steps), because of the addition of the new taxa (*Camarillasaurus*, *Limusaurus*). Tree statistics are Consistency Index, CI = 0.668, Retention Index, RI = 0.784, and Rescaled Consistency Index, RC = 0.524. The majority-rule consensus tree (Fig. 12A) is similar to the findings of Carrano and Sampson (2008: fig. 4) in distinguishing Ceratosauria from the three outgroup taxa (*Herrerasaurus*, *Syntarsus*, *Allosaurus*), and in separating the two families of Abelisauoidea, the Abelisauridae, and Noasauridae. Further, the Noasauridae are an unresolved polytomy, whereas Abelisauridae shows the same arrangement of taxa as in Carrano and Sampson (2008: fig. 4). *Limusaurus* is identified as the basalmost member of Ceratosauria, followed by *Camarillasaurus*, outside Abelisauoidea. The bootstrap result (Fig. 12B) shows the complete collapse of all ceratosaurs into a large unresolved multitomy, in which *Camarillasaurus* participates, with *Limusaurus* as sister group, and the outgroups are reasonably securely distinguished. Results shown here (Fig. 12A) are from the TNT “new technology” searches, and they differ from the PAUP results only in minor ways: in the PAUP majority-rule tree, *Deltadromeus* forms an unresolved polytomy with (*Spinostropheus*–*Elaphrosaurus*) and remaining members of Ceratosauria, rather than with *Camarillasaurus*, and *Abelisaurus* is sister to (*Rajasaurus*–*Indosaurus*–*Majungasaurus*) rather than being unresolved with the other carnosaurine abelisaurids (Fig. 12A).

In the second analysis, we pruned some taxa to improve resolution: Carrano and Sampson (2008: 199) found that three genera, *Deltadromeus*, *Abelisaurus*, and *Aucasaurus*, acted as “wildcard” taxa, being placed at the bases of resolved nodes and reducing them to polytomies. The run of the pruned data matrix, but with *Camarillasaurus* and *Limusaurus* added, did not change the topology of the resultant consensus tree, except that the three pruned taxa were deleted, and our tree statistics were comparable to those found by the original authors (264 trees of length 234 steps, CI = 0.688, RI = 0.775; RC = 0.533). However, when run in TNT, which takes a stricter approach to collapsing branches (Goloboff et al. 2008), fewer trees are often found, and in this case, a single tree was produced (Fig. 12C). *Limusaurus* remains the basalmost ceratosaur, followed by *Camarillasaurus*, *Ilokelesia*, and *Carnotaurus* are paired as sister taxa, as are *Elaphrosaurus* and *Spinostropheus*, and *Majungasaurus* and *Rajasaurus*. Further, and interestingly, the Noasauridae are completely resolved, unlike any other analysis, here or by Carrano and Sampson (2008), with *Laevisuchus* and *Masiakasaurus* paired as most derived members of the clade. However, many of these resolved nodes collapse when the data are subjected to bootstrapping (Fig. 12D), *Elaphrosau-*

rus and *Spinostropheus* retain their pairing, but the abelisaurid subclades and the Noasauridae become a single unresolved multitomy. *Limusaurus* and *Camarillasaurus* are still most basal ceratosaurians, but with only 20% and 18% bootstrap support, and so these nodes collapse into the single ceratosaurian multitomy.

Conclusions

Camarillasaurus cirugedae from the Lower Cretaceous (Barremian) of Spain is identified as a new ceratosaurian theropod, based on two apomorphies, the great development of the cnemial crest area, giving an extremely deep tibial proximal end, and the deep, longitudinal groove on the tibia.

In phylogenetic analysis, *Camarillasaurus* is a basal ceratosaur, perhaps more derived than *Limusaurus*, but the incompleteness of the Spanish material means very few characters could be coded (only 17 of 151) and so its position might change with fuller coding.

Camarillasaurus cirugedae is the first ceratosaur described from the Iberian Peninsula, and the second from Europe, after the abelisauroid *Genusaurus*. Its importance is in partially filling the earliest Cretaceous “ceratosaur gap”, a time of limited fossils. With such an incompletely resolved phylogeny, the geographic distribution of ceratosaurs, with finds through the Jurassic and Cretaceous in Europe, North America, Africa, Asia, and South America has become more complex than at a time when the clade was seen as largely Gondwanan in distribution in the Cretaceous.

Acknowledgements

We thank Pedro Cirujeda Buj (Camarillas, Spain) and José María Herrero (Galve, Spain) for access to the material, Simon Powell (Bristol University, UK) for his help with photography, and Bárbara Martínez (Curator of the Museo Numantino of Soria, Spain) for her useful advice about the preparation of the bones. We thank Xu Xing (Institute of Vertebrate Paleontology and Paleoanthropology, Beijing, China) for permission to examine the type specimen of *Limusaurus*. Many thanks to Octávio Mateus (Museu da Lourinhã, Portugal), for his comments about the *Ceratosaurus* material from Portugal and to Matt Carrano (Smithsonian Institution, Washington DC, USA) and Ronald Tykoski (Museum of Nature and Science, Dallas, Texas) for other advice. We are especially grateful to Jonah Choiniere (American Museum of Natural History, New York, USA), and an anonymous reviewer for their useful comments and review of earlier versions of this manuscript.

References

- Accarie, H., Beaudoin, B., Dejax, J., Friès, G., Michard, J.-G., and Taquet, P. 1995. Découverte d'un dinosaure théropode nouveau (*Genusaurus susteronis* n. g., n. sp.) dans l'Albien marin de Sisteron (Alpes de Haute-Provence, France) et extension au Crétacé inférieur de la lignée cératosaurienne. *Compte Rendus de l'Académie des Sciences, Paris, Série IIa* 320: 327–334.

- Formation, with a description of a new species of *Criquetulus*. *Pgy "Ogzlek'Owugwo 'qhl'Pcwt'crl'J knqt {'cpf'Uelkpeg'Dwngkp 36: 1–7.*
- Molnar, R.E., Kurzanov, S.M., and Dong, Z.-M. 1990. Carnosauria. *Kp: D.B. Weishampel, P. Dodson, and H. Osmólska (eds.), Vj g'Fkpqucw' tlc, 169–209.* University of California Press, Berkeley.
- Naish, D. 2003. A definitive allosauroid (Dinosauria; Theropoda) from the Lower Cretaceous of East Sussex. *Rtqeggf'kpi u'qhl'j g'T gqrqi knuð'Cu' uqek'vkpp 113: 153–163.*
- Novas, F.E., Souza Carvalho, I. de, Borges Ribeiro, L.C., and Méndez, A.H. 2008. First abelisaurid bone remains from the Maastrichtian Marília Formation, Bauru Basin, Brazil. *"Etvgeqqu'Tgugctej 29: 625–635.*
- O'Connor, P.M. 2006. Postcranial pneumaticity: an evaluation of soft-tissue influences on the postcranial skeleton and the reconstruction of pulmonary anatomy in archosaurs. *Lqwt'pcrl'qhl'O qtr'j qnqi { 267: 1199–1226.*
- O'Connor, P.M. 2007. The postcranial axial skeleton of *Ochlopi cucwt'wu' etgpc'vkuo wu* (Theropoda: Abelisauridae) from the late Cretaceous of Madagascar. *O'go qk' "qhl'j g'Uelk'v' "qhl'Xgt'v'gdt'cv'g'Rcrg'qpv'qni { 8: 127–162.*
- Ostrom, J. H. 1969. Osteology of *Fg'lp'p'f'ej wu'cpv't'j qrwu*, an unusual theropod from the Lower Cretaceous of Montaña. *Rgc'dqf {"Owugwo " qhl'Pcwt'crl'J knqt {'Dwngkp 30: 1–165.*
- Pol, D. and Rauhut, O.W.M. 2012. A Middle Jurassic abelisaurid from Patagonia and the early diversification of theropod dinosaurs. *Rtqeggf' kpi u'qhl'j g'Tq'crl'Uelk'v' "Ugt'kgu'D'279: 3170–3175.*
- Rauhut, O.W.M. 2003. The interrelationships and evolution of basal theropod dinosaurs. *U'g'ek'rl'Rcr'gtu'lp'Rcrg'qpv'qni { 69: 1–213.*
- Rauhut, O.W.M. 2004. Provenance and anatomy of *I gp'f'qf'gevu'ugt'wu*, a large-toothed ceratosaur (Dinosauria: Theropoda) from Patagonia. *Lqwt'pcrl'qhl'Xgt'v'gdt'cv'g'Rcrg'qpv'qni { 24: 894–902.*
- Rauhut, O.W.M. 2005a. Osteology and relationships of a new theropod dinosaur from the Middle Jurassic of Patagonia. *Rcrg'qpv'qni { 48: 87–110.*
- Rauhut, O.W.M. 2005b. Post-cranial remains of "coelurosaur" (Dinosauria, Theropoda) from the Late Jurassic of Tanzania. *I gqrqi ke'crl'O'ci/ c'kpg 142: 97–107.*
- Rauhut, O.W.M. 2011. Theropod dinosaurs from the Late Jurassic of Tendaguru (Tanzania). *U'g'ek'rl'Rcr'gtu'lp'Rcrg'qpv'qni { 86: 195–239.*
- Rauhut, O.W.M. 2012. A reappraisal of a putative record of abelisauroid theropod dinosaur from the Middle Jurassic of England. *Rtqeggf'kpi u' qhl'j g'T gqrqi knuð'Cu'qek'vkpp 123: 779–786.*
- Rauhut, O.W.M. and Xu, X. 2005. The small theropod dinosaurs *Vui w' nu'cw'wu* and *Rj'c'g'f't'q'nc'wt'wu* from the Early Cretaceous of Xingjiang, China. *Lqwt'pcrl'qhl'Xgt'v'gdt'cv'g'Rcrg'qpv'qni { 25: 107–118.*
- Rauhut, O.W.M., Cladera, G., Vickers-Rich, P.A., and Rich, T.H. 2003. Dinosaur remains from the Lower Cretaceous of the Chubut Group, Argentina. *Etvgeqqu'Tgugctej 24: 487–497.*
- Rogers, R.R., Krause, D.W., and Rogers, K.C. 2003. Cannibalism in the Madagascan dinosaur *Ochlopi cvj qnu'ev'qrwu*. *Pcwt'g'422: 515–518.*
- Salas, R. and Casas, A. 1993. Mesozoic extensional tectonics, stratigraphy and crustal evolution during the Alpine cycle of the Eastern Iberian Basin. *Vge'v'q'p'q'r'j {t'keu 228: 33–55.*
- Sánchez-Hernández, B. 2002. Asociación faunística de vertebrados mesozoicos de la localidad de Galve (Teruel). *Gnw'f'kqu'T gqrwi'kequ 58: 189–193.*
- Sánchez-Hernández, B. 2005. *I c'rk'q'uc'wt'wu'j g't'gt'q'k*, a new sauropod dinosaur from Villar del Arzobispo Formation (Tithonian–Berriasian) of Spain. *\ qqw'zc 1034: 1–20.*
- Sánchez-Hernández, B., Benton, M.J., and Naish, D. 2007. Dinosaurs and other fossil vertebrates from the Late Jurassic and Early Cretaceous of the Galve area, NE Spain. *Rcrg'q'gi'g'qi't'cr'j'f' "Rcrg'q'ger'ko'cv'q'ni'f' " Rcrg'q'g'e'q'ni'f' 249: 180–215.*
- Schubert, B.W. and Ungar, P.S. 2005. Wear facets and enamel spalling in tyrannosaurid dinosaurs. *Cev' "Rcrg'q'p'v'q'ni'k'ec' "R'q'rp'k'ec 50: 93–99.*
- Seeley, H.G. 1887. The classification of the Dinosauria. *T'gr'qt'v'qhl'j'g' "Dt'k'v' k'ij' "Cu'q'ek'vk'p' "l'qt' "j'g' "C'f'xc'p'ego'g'p'v'qhl'Uelk'peg 1887: 698–699.*
- Sereno, P.C. 1999. The evolution of dinosaurs. *Uelk'peg 284: 2137–2147.*
- Sereno, P.C. and Brusatte, S.L. 2008. Basal abelisaurid and carcharodontosaurid theropods from the Lower Cretaceous Elrhaz Formation of Niger. *Cev' "Rcrg'q'p'v'q'ni'k'ec' "R'q'rp'k'ec' 53: 15–46.*
- Sereno, P.C., Wilson, J.A., and Conrad, J.L. 2004. New dinosaurs link southern landmasses in the Mid-Cretaceous. *Rtq'eg'gf'k'pi' u'qhl'j'g' "T'q'c'rl' Uelk'v' "qhl'N'q'p'f'q'p' "Ugt'kgu'D'271: 1325–1330.*
- Smith, J.B., Lamanna, M.C., Askar, A.S., Bergig, K.A., Tshakreen, S.O., Abugares, M.M., and Rasmussen, D.T. 2010. A large abelisauroid theropod dinosaur from the early Cretaceous of Libya. *Lqwt'pcrl'qhl'Rc/ rg'q'p'v'q'ni'f' 84: 922–934.*
- Smith, J.B., Vann, D.R., and Dodson, P. 2012. Dental morphology and variation in theropod dinosaurs: Implications for the taxonomic identification of isolated teeth. *Vj'g' "C'p'c'v'q'o'ke'crl'T'ge'q'f' 285A: 699–736.*
- Soria, A.R. 1997. *Nc' "ug'f'ko'g'p'v'ek'p' "gp' "rc'u'ew'g'p'ecu'o'c'ti'k'p'c'ru'f'g'gr'w'at'eq" k'd'2't'ke'q' "f'w'c'p'v'g' "gr' "Et'g'v' "ek'eq' "k'p'g't'k'qt' "f' "w'w'eq'p'v'q'nt'g'ut'c'w'i't' "h'ek'q. 363 pp.* Doctoral thesis, Universidad de Zaragoza, Zaragoza.
- Swofford, D.L. 2002. PAUP*. *Rj' {r'qi'g'p'v'ke' "C'p'c'rl'ukt' "W'ik'p'i' "R'ct'uko'q'p'f' " *; c'p'f' "Q'j'g't' "O'g'v'q'f' u' "X'gt'uk'q'p' "6.* Sinauer Associates, Sunderland, Massachusetts.
- Tykoski, R.S. and Rowe, T. 2004. Ceratosauria. *Kp: D.B. Weishampel, P. Dodson, and H. Osmólska (eds.), Vj'g' "F'kp'qu'cw' tlc, 47–70.* University of California Press, Berkeley.
- Welles, S.P. 1984. *F'k'q'r'j'q'uc'wt'wu' "y'g'j'g't'k'k'k' (Dinosauria, Theropoda), osteology and comparisons. Rcrg'q'p'v'q'ni't'cr'j'k'ec' "C'd'v'g'h'w'p'i' "CU 185: 85–180.*
- Wilson, J.A., Sereno, P.C., Srivastava, S., Bhatt, D.K., Khosla, A., and Sahni, A. 2003. A new abelisaurid (Dinosauria: Theropoda) from the Lameta Formation (Cretaceous, Maastrichtian) of India. *Eq'p'v'k'bw'k'q'p'u' "h'q'o' "j'g' "O'wugwo' "qhl'Rcrg'q'p'v'q'ni'f' "W'p'k'c'g't'uk'of' "qhl'O'ke'j'k'i'c'p' 31: 1–42.*
- Xu, X., Clark, J.M., Mo, J., Choiniere, J., Forster, C.A., Erickson, G.M., Hone, D.W.E., Sullivan, C., Eberth, D.A., Nesbitt, S., Zhao, Q., Hernandez, R., Jia, C.-K., Han, F.-L., and Guo, Y. 2009. A Jurassic ceratosaur from China helps clarify avian digital homologies. *Pcwt'g'459: 940–944.*